BIOCHEMISTRY
including biophysical chemistry & molecular biology

Article

pubs.acs.org/biochemistry

# A Calorimetric and Spectroscopic Comparison of the Effects of Lathosterol and Cholesterol on the Thermotropic Phase Behavior and Organization of Dipalmitoylphosphatidylcholine Bilayer Membranes

Matthew G. K. Benesch, David A. Mannock, Ruthven N. A. H. Lewis, and Ronald N. McElhaney*

Department of Biochemistry, School of Translational Medicine, Faculty of Medicine and Dentistry, University of Alberta, Edmonton, Alberta, Canada T6G 2H7

**ABSTRACT:** We performed differential scanning calorimetry (DSC) and Fourier transform infrared (FTIR) spectroscopic measurements to study the effects of lathosterol (Lath) on the thermotropic phase behavior and organization of dipalmitoylphosphatidylcholine (DPPC) bilayer membranes and compared our results with those previously reported for cholesterol (Chol)/DPPC binary mixtures. Lath is the penultimate intermediate in the biosynthesis of Chol in the Kandutsch−Russell pathway and differs from Chol only in the double bond position in ring B, which is between C7 and C8 in Lath and between C5 and C6 in Chol. Our DSC studies indicate that the incorporation of Lath is more effective than Chol in reducing the temperature and enthalpy of the DPPC pretransition. At lower sterol concentrations (≤10 mol %), incorporation of both Lath and Chol decreases the temperature, enthalpy, and cooperativity of the sharp component of the main phase transition of DPPC to a similar extent, but at higher sterol concentrations, Lath is more effective at decreasing the phase transition temperature, enthalpy, and cooperativity than Chol. These results indicate that at higher concentrations, Lath is more disruptive of DPPC gel-state bilayer packing than Chol is. Moreover, incorporation of Lath decreases the temperature of the broad component of the main phase transition of DPPC, whereas Chol increases it; this difference in the direction and magnitude of the temperature shift is accentuated at higher sterol concentrations. Although at sterol concentrations of ≤20 mol % Lath and Chol are almost equally effective at reducing the enthalpy and cooperativity of the broad component of the main phase transition, at higher sterol levels Lath is less effective than Chol in these regards and does not completely abolish the cooperative hydrocarbon chain melting phase transition at 50 mol %, as does Chol. These latter results indicate that Lath both is more disruptive with respect to the low-temperature state of the sterol-enriched domains of DPPC bilayers and has a lower lateral miscibility in DPPC bilayers than Chol. Our FTIR spectroscopic studies suggest that Lath incorporation produces a less tightly packed bilayer than does Chol at both low (gel state) and high (liquid-crystalline state) temperatures, which is characterized by increased H-bonding between water and the carbonyl groups of the fatty acyl chains in the DPPC bilayer. Overall, our studies indicate that Lath and Chol incorporation can have rather different effects on the thermotropic phase behavior and organization of DPPC bilayers and thus that the position of the double bond in ring B of a sterol molecule can have an appreciable effect on the physical properties of sterol molecules.

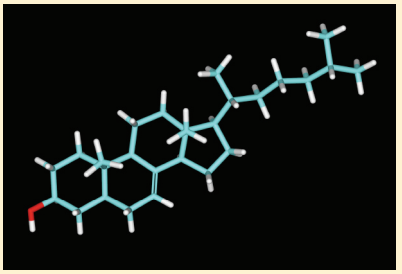

Cholesterol (Chol) is a major and essential lipid component of the plasma membranes of the cells of higher animals and is also found in lower concentrations in certain intracellular membranes in vesicular communication with the plasma membrane (see refs 1−3). Although Chol has a number of different functions in animal cells, one of its primary roles is as a modulator of the physical properties and lateral organization of the plasma membrane lipid bilayer. Thus, many studies of the interaction of Chol with phospholipid monolayer and bilayer model membranes have been performed, utilizing a wide range of physical techniques.[2,4−7] Most of those studies have utilized symmetrical chain, linear saturated PCs. They have established that one of the major effects of the incorporation of Chol on phospholipid monolayer and bilayer model membranes is a broadening and eventual elimination of the cooperative gel-to-liquid-crystalline phase transition and its replacement by a state with an intermediate degree of organization. Thus, in the liquid-crystalline phase, which would exist at physiological temperatures in the absence of sterols in biological membranes, the presence of Chol significantly increases the orientational order of the phospholipid hydrocarbon chains and decreases the cross-sectional area occupied by the phospholipid molecules, while only moderately restricting the rates of phospholipid lateral diffusion or hydrocarbon chain motion. In addition, the presence of Chol increases both the thickness and mechanical strength and decreases the permeability of the phospholipid bilayer in the physiologically relevant liquid-crystalline phase. The relatively high rates of intramolecular and intermolecular motion characteristic of phospholipid model

**Received:** May 10, 2011
**Revised:** September 26, 2011
**Published:** September 27, 2011

membranes in the presence of high levels of Chol, coupled with an increased hydrocarbon chain order and a decreased area compressibility, have prompted several researchers to postulate the existence of a discrete liquid-ordered ($l_o$) phase in binary phospholipid/Chol model membranes.[5,8,9] However, as many of the physical properties of model membranes composed of Chol and a single phospholipid change smoothly and monotonically with progressive increases in Chol concentration up to 50 mol %,[2,4−7] the existence of thermodynamically discrete, macroscopic $l_d$ and $l_o$ phases in such binary systems has been questioned,[7,10,11] and it has been suggested that the behavior of phospholipid/Chol systems can be explained by the formation of various superlattices[12] or molecular complexes.[13] However, in model membranes composed of Chol, unsaturated PCs, and natural SpMs, the specificity of the interaction of Chol for SpM can result in the formation of macroscopic domains enriched in Chol and SpMs and depleted of unsaturated PCs, and such domains are thought to form the molecular basis for the possible existence of detergent-insoluble, Chol- and SpM-enriched lipid rafts in biological membranes.[14−19] Even in such ternary systems, however, the existence of thermodynamically discrete $l_d$ and $l_o$ systems has not been detected by DSC or X-ray diffraction,[20] and a number of researchers have found evidence of the existence of relatively large, long-lived lipid rafts in biological membranes unconvincing.[21−23] Whatever the biophysical details, it is clear that the presence of Chol in biological membranes does modulate a number of different membrane functions, either directly or via its effects on the properties and lateral organization of the phospholipid bilayer.[2,24−26]

Chol is by far the predominate sterol in the membranes of higher animals, and the later biosynthetic intermediates in its long and energetically costly biosynthetic pathway do not normally accumulate in the membranes of healthy cells.[24] There are two major pathways for Chol biosynthesis starting from lanosterol, the first cyclic intermediate formed in the biosynthesis of all sterols, the Kandutsch−Russell[27] and Bloch[28] pathways. K. Bloch proposed that these sterol biosynthetic pathways reflect sterol evolution, with the structure of the Chol molecule having been evolutionarily selected to optimize certain biophysical properties of the lipid bilayers of the host cell membrane into which they are embedded, such as those briefly discussed above. According to this hypothesis, Chol biosynthetic precursors should exhibit physical effects on host lipid bilayers that more effectively support membrane structure and function as one progresses along these biosynthetic pathways toward Chol (ref 28, but see ref 29). Comparative studies of the effects of Chol and its biosynthetic precursors on the physical properties of lipid bilayer model membranes are of obvious relevance to determining the validity of the Bloch hypothesis.

Lath is the next-to-last intermediate in the Kandutsch−Russell pathway of Chol biosynthesis and is the biosynthetic intermediate in both pathways whose chemical structure is most similar to that of Chol itself. In fact, as illustrated in Figure 1, the structures of Lath and Chol are identical except for the position of the single double bond in ring B, which is located between C7 and C8 in Lath and C5 and C6 in Chol. Despite their very similar chemical structures and physical properties, defects in the Kandutsch−Russell biosynthetic pathway that result in the accumulation of Lath give rise to lathosterolosis, a serious and usually fatal mammalian malformation syndrome characterized by multiple congenital abnormalities, mental

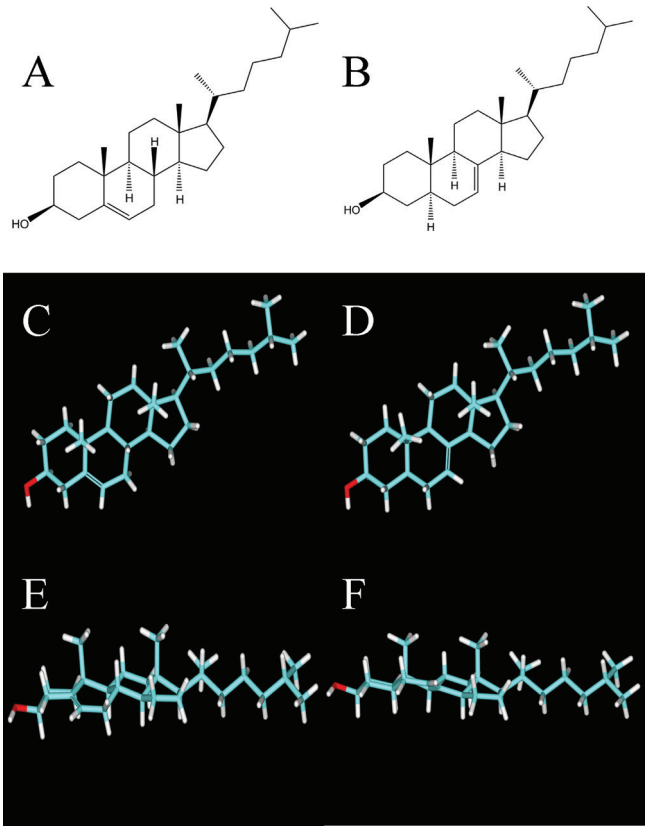


**Figure 1.** Molecular models for cholesterol and lathosterol. The top row shows line diagrams to highlight differences between the structures of the cholesterol (A) and lathosterol (B) molecules. The middle row shows views normal to the plane of the sterol ring for cholesterol (C) and lathosterol (D), and the bottom row shows views parallel to the plane of the sterol ring for cholesterol (E) and lathosterol (F). The hydroxyl group at C3 is colored red. The molecules were minimized using DSViewer Pro 6.0 (Accelrys Software Inc., San Diego, CA).

retardation, and mental disease.[30−33] The balance of evidence suggests that the development of lathosterolosis is due to perturbed signaling by the sonic hedgehog morphogenic system, which plays a major role in embryonic development, and that this perturbation is due primarily to the reduced level of Chol present in affected individuals, rather than from the accumulation of Lath itself.[32,33] However, a recent study found that Lath and other late intermediates in the Chol biosynthetic pathways preferentially accumulate in operationally defined lipid rafts, where they may disrupt lipid raft organization and thus interfere with lipid raft-mediated signaling more generally.[34] Moreover, in lathosterolotic mice, the numbers of functional secretory granules in the pancreas and adrenal and pituitary glands are markedly diminished but can be restored to normal numbers, morphology, and function by the replacement of accumulated Lath by exogenous Chol.[35] This study also determined that incorporation of Lath into lipid model membranes decreases their bending rigidty and intrinsic curvature, which was suggested to account for the effect of Lath accumulation in abnormal granule budding in these glands. Moreover, a study of the comparative effects of Lath and Chol on the rate of PC biosynthesis, and the activity of CTP:phosphocholine cytidylyl transferase, the rate-limiting enzyme in this pathway, demonstrated that Lath was much less effective than Chol in supporting PC biosynthesis and

stimulating the activity of this enzyme. This effect was suggested to be due to the dependence of CTP:phosphocholine cytidylyl transferase activity on the intrinsic curvature of the lipid bilayer in which this membrane-associated enzyme is embedded, which is differentially affected by these two sterols.[36] Therefore, whether the accumulation of Lath (and other Chol biosynthetic precursors) is inherently toxic, adversely affecting membrane (and possibly other) functions, either directly or indirectly, whether a deficiency of Chol is ultimately responsible for the loss of cell viability, or whether both effects play a role remains an open question.

The results of the limited number of comparative studies of the physical properties of Lath and Chol, and their effects on phospholipid bilayers, vary considerably and are not always in agreement with one another. Stottrup and Keller[37] report that although the cross-sectional areas of both sterols are the same at their collapse pressures in pure sterol monolayer films, Lath monolayers exhibit a considerably higher collapse pressure than do those of Chol, suggesting that Lath−Lath interactions are stronger than Chol−Chol interactions. Although both sterols are "membrane-active" (can produce monolayers containing two distinct immiscible liquid phases in ternary DOPC/DPPC/sterol systems), Lath/DPPC binary mixtures do not exhibit such phase separation at lower sterol concentrations, whereas Chol/DPPC monolayers do. These workers also report that Lath is more effective than Chol in condensing and rigidifying DPPC monolayers at 30 mol % sterol, but less effective at 50 mol % sterol. This latter result, which suggests that Lath is not as laterally miscible in phospholipid bilayers as Chol, supports the results of this study, as discussed below.

Nyholm et al.[38] have also conducted a comparative DSC study of binary mixtures of Lath and Chol with PSM and PDHSM, or with mixtures of these sphingolipids with DPPC, over a range of sterol concentrations from 0 to 25 mol % in 5 mol % increments. In general, the effects of Lath and Chol on the thermotropic phase behavior of these binary or ternary mixtures were reported to be quite similar. In particular, the addition of either sterol at 10 mol % abolished the pretransition of PSM and PDHSM. Moreover, the addition of larger amounts of either sterol decreased the temperature, enthalpy, and cooperativity of the sharp component of the main phase transition, arising from the sphingolipid hydrocarbon chain melting of the sterol-poor domain. At the same concentration, each sterol increased the temperature but decreased the enthalpy and cooperativity of the broad component of the phase transition, originating from the melting of sterol-rich domains in the sphingolipid bilayer. In general, these results resemble those reported here for sterol/DPPC binary mixtures.

Ranadive and Lala[39] conducted a comparative study of the effects of the incorporation of a number of double bond isomers of Chol, including Lath, on the glucose permeability and their ability to order egg PC vesicles using electron spin resonance and fluorescence polarization spectroscopy. These workers report that Lath is only approximately half as effective as Chol in reducing glucose permeability and in increasing the order of both the hydrocarbon core and interfacial regions of the host egg PC bilayers. However, Oradd et al.,[40] utilizing $^2$H NMR spectroscopy, found no significant difference in the ability of Lath and Chol to order the terminal $CD_3$ group of hydrocarbon chain-perdeuterated DMPC and DPPC bilayers or to increase their bending rigidity. In contrast, using X-ray diffraction and an osmotic stress technique, Petrache et al.[41] reported that Lath is considerably less effective than Chol in eliminating thermally induced undulations in DMPC bilayers, indicating lower bilayer stiffness in Lath- versus Chol-containing vesicles. Moreover, they also reported that incorporation of Lath induces the formation of a reversed hexagonal phase with a larger diameter in DOPE dispersions versus that produced by Chol, indicating that Lath incorporation produces a lower intrinsic curvature. This interpretation is supported by the results of Leppimaki et al.,[36] who found by DSC that Lath incorporation reduces the lamellar−nonlamellar phase transition temperature of POPE dispersions to a lesser extent than Chol, suggesting that Lath has a less pronounced inverted conical shape than Chol, because it less effectively destabilizes the lamellar phase relative to the reversed phase (see also ref 42). Finally, several groups, using a variety of different physical techniques, all report that Lath is actually slightly more effective than Chol in inducing the $l_o$ phase in ternary lipid mixtures, and that Lath-induced $l_o$ phases have slightly greater thermal stability than Chol-induced $l_o$ phases.[43−45] Thus, Lath should be at least as effective in supporting lipid raft formation in biological membranes as Chol.

This brief summary demonstrates that the number of comparative biophysical studies of the effects of Lath and Chol on the structure and properties of lipid model membranes is relatively limited and that the results of some of these studies disagree. To investigate the interactions between Lath and model membrane bilayers and thus the potential biophysical contributions of Lath to the membrane-associated processes mentioned above, we have performed a comparative DSC study of the effects of the incorporation of a wide range of concentrations of Lath on the thermotropic phase behavior of well-studied DPPC model membranes using high-sensitivity calorimeters and an experimental protocol that ensures that the broad, low-enthalpy phase transitions occurring at high sterol concentrations are accurately monitored. This thermodynamic approach, together with supporting FTIR measurements, allows the comparison of the thermotropic phase behavior and organization of DPPC mixtures containing a range of sterols differing in the chemical configuration of the steroid nucleus. In this study, we compare our results for Lath/DPPC mixtures with those obtained for Chol and related Chol analogues in DPPC-containing mixtures, which we reported previously.[46−50] In general, our results indicate that Lath and Chol have similar but not identical effects on lipid bilayer model membranes at low sterol concentrations. However, significant differences in the thermodynamic parameters become evident at higher, physiologically relevant sterol concentrations.

## MATERIALS AND METHODS

DPPC, DPPC-$d_{62}$, and Chol (5-cholesten-3$\beta$-ol) were all obtained from Avanti Polar Lipids Inc. (Alabaster, AL), whereas the Lath (7-cholesten-3$\beta$-ol) was supplied by Steraloids Inc. (Newport, RI). The purities of both DPPCs and Chol were >99%, and Lath was >98% pure. All organic solvents were of at least analytical grade quality and were redistilled before use. Samples for hydration were prepared exactly as described previously.[46] The sterol/DPPC films were subsequently dispersed in an appropriate volume of deionized water by vigorous vortex mixing at temperatures near 55−60 °C. This procedure prevents any fractional crystallization of the sterol during sample preparation.

**Differential Scanning Calorimetry.** The samples used for the DSC experiments were prepared by dispersing

appropriate amounts of the dried sterol/lipid mixture in 1 mL of deionized water. The dispersion was then degassed, and either 900 $\mu$L (for studying the main phase transition) or 324 $\mu$L (for studying the pretransition) aliquots were withdrawn for DSC analyses. To ensure better resolution of the broad low-enthalpy thermotropic transitions exhibited by sterol-rich mixtures, the amount of lipid used for DSC measurements was progressively increased with the sterol content of the mixture.[51,52] Typically, samples containing 1−3 mg of phospholipid were used at sterol concentrations below 5 mol %, samples containing 5−8 mg of phospholipid at sterol concentrations between 5 and 15 mol %, and samples containing 25 mg of phospholipid at all higher sterol concentrations. DSC heating and cooling thermograms were obtained at a scan rate of 10 °C/h using a either a Hart multicell high-sensitivity DSC instrument for the main phase transition measurements or a high-sensitivity Nano II DSC instrument for the pretransition measurements (both instruments were supplied by Calorimetry Sciences Corp., Lindon, UT). The data acquired were analyzed and plotted with Origin version 7.5 Pro (OriginLab Corp., Northampton, MA). In cases where the DSC thermograms appeared to be a summation of overlapping components, the midpoint temperatures, areas, and widths of the components were estimated with the aid of the Origin nonlinear least-squares curve- and peak-fitting procedures and a custom-coded function based on the assumption that the observed thermogram was a linear combination of components, each of which could be approximated by a reversible two-state transition at thermodynamic equilibrium.[52] In strict terms, the treatment of the sharp and broad components of the multicomponent endotherms as independent events is not entirely justified, as these two processes may be coupled thermodynamically. However, at present no rigorous alternative method for deconvolving obviously multicomponent endotherms exists.

**Fourier Transform Infrared (FTIR) Spectroscopy.** Samples used for FTIR spectroscopic experiments were prepared by dispersing dried DPPC and sterol/lipid mixtures containing 2−3 mg of phospholipid in 50 $\mu$L of $D_2O$ at approximately 55−60 °C. The paste so formed was then sealed as a thin (25 $\mu$m) film between the $CaF_2$ windows of a heatable, demountable liquid cell equipped with a 25 $\mu$m Teflon spacer. The temperature of the sample was controlled between 0 and 60 °C using an external, computer-controlled water bath. The FTIR spectra were recorded with a Digilab FTS-40 Fourier transform spectrometer (Bio-Rad, Digilab Division, Cambridge, MA) using data acquisition and data processing protocols described by Lewis et al.[53]

The sterol-containing samples used for FTIR spectroscopy contained 30 mol % sterol, levels that are high enough to avoid ambiguities attributable to the coexistence of sterol-rich and sterol-poor DPPC domains but low enough to ensure that Lath is still fully miscible in the DPPC bilayer and that the samples will also exhibit calorimetrically resolvable phase transitions that can be compared with those recorded in our DSC studies. Studies were also performed with samples derived from normal (i.e., fully protonated) DPPC and its chain-perdeuterated analogue, DPPC-$d_{62}$. With the sterol-rich samples derived from normal DPPC, absorption bands in the C−H stretching region of the IR spectrum will contain a significant contribution from the C−H groups on the sterol. However, because the sterol does not participate in the phospholipid hydrocarbon chain-melting phase transition, there may be some uncertainty in interpreting the frequencies of these bands in terms of the degree of hydrocarbon chain conformational order existing in the various samples examined. The use of the DPPC-$d_{62}$ analogue prevents such problems, because the relevant C−D stretching bands occur at frequencies between 2050 and 2250 $cm^{-1}$ (ref 54 and references cited therein), well away from the frequency range of C−H stretching vibrations and from those of other functional groups present in these lipids. However, one should also note that the gel to liquid-crystalline phase transition temperature of DPPC-$d_{62}$ is ∼3−4 °C lower than that of fully proteated DPPC,[55] and as a result, the transition temperatures of the corresponding sterol-containing samples will be somewhat lower than those of the corresponding mixtures made with protonated DPPC.

## RESULTS

**Differential Scanning Calorimetry Measurements of the Thermotropic Phase Behavior of Lathosterol/DPPC Mixtures.** In this study, we use our previously published measurements of Chol/DPPC binary mixtures[46] as reference data for a comparison with the new DSC and FTIR spectroscopy measurements of the Lath/DPPC mixtures. Figure 2 shows DSC heating scans of DPPC dispersions

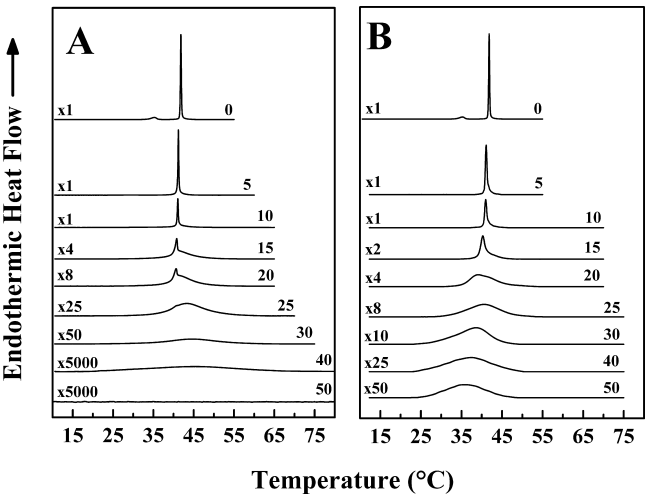


**Figure 2.** DSC thermograms illustrating the effect of cholesterol (A) and lathosterol (B) on the gel to liquid-crystalline phase transition of DPPC. The thermograms shown were acquired at the sterol concentrations (mole percent) indicated at a scan rate of 10 °C/h and have all been normalized against the mass of DPPC used. *Y*-Axis scaling factors are indicated on the right side of each thermogram.

containing differing concentrations of both sterols. The overall pattern of thermotropic phase behavior seen upon heating is broadly similar to that reported previously for Chol/DPPC and other sterol/DPPC binary mixtures.[47−50,56] Pure DPPC heating scans show two sharp endothermic peaks centered at 35 and 41.7 °C, which correspond to the pretransition ($L_{\beta}'$ to $P_{\beta}'$) and main ($P_{\beta}'$ to $L_{\alpha}$) phase transitions, respectively. Increasing the sterol concentration gradually broadens the pretransition and reduces its temperature, enthalpy, and cooperativity in both cases. Similarly, in the case of the main phase transition, increasing the sterol concentration initially produces a multicomponent DSC endotherm, consisting of a sharp component that progressively undergoes decreases in temperature, enthalpy, and cooperativity and a broad component that

undergoes increases in both temperature and enthalpy but decreases in cooperativity. Thus, with increasing sterol concentrations, the sharp component disappears as the broad component grows. However, there are subtle but significant differences in the pattern of thermal events observed in the Chol/DPPC (Figure 2A) and Lath/DPPC (Figure 2B) samples, which indicate that the behavior of the latter is quantitatively different from the former, despite their similar chemical structures. We will first focus on the effect of both sterols on the pretransition and then on the two deconvolved components of the main phase transition of DPPC.

**Effects of Lathosterol on the Pretransition of DPPC.** To investigate the disappearance of the pretransition in greater detail, we prepared sterol/DPPC samples with a narrower range of sterol concentrations. Heating thermograms obtained from DPPC mixtures containing Chol (Figure 3A) and Lath

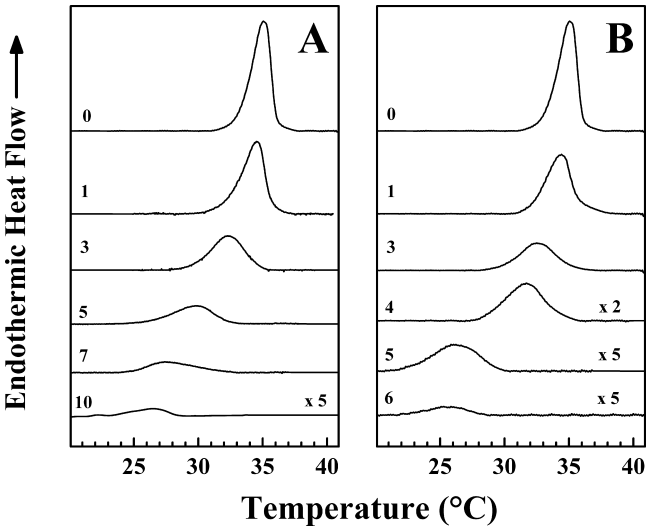


**Figure 3.** DSC thermograms illustrating the effect of cholesterol (A) and lathosterol (B) on the pretransition of DPPC. The thermograms shown were acquired at the sterol concentrations (mole percent) indicated at a scan rate of 10 °C/h and have all been normalized against the mass of DPPC used. *Y*-Axis scaling factors are indicated on the left side of each thermogram.

(Figure 3B) both show generally similar decreases in $T_p$ and $\Delta H_p$ and increases in $\Delta T_{1/2}$ with an increasing sterol concentration, although Lath abolishes the DPPC pretransition at lower concentrations than does Chol. The corresponding thermodynamic measurements for both sterol/DPPC systems are presented in Figure 4. The Lath/DPPC and Chol/DPPC samples show comparable decreases in $T_p$ (Figure 4A) with an increasing sterol concentration up to sterol concentrations of ~4 mol %. Above that concentration, the $T_p$ of the Lath/DPPC mixtures decreases abruptly by 7 °C between 4 and 6 mol % sterol. In contrast, Chol/DPPC mixtures show a smaller decrease in $T_p$ at 4 mol % sterol, which decreases by 6 °C over a concentration range from 4 to 10 mol % Chol, suggesting a similar change in the pretransition properties is distributed over a wider range of Chol concentrations.

Corresponding plots of the $\Delta T_{1/2}$ values obtained from DPPC mixtures containing either Lath or Chol are shown in Figure 4B. The values obtained for the Chol- and Lath-containing DPPC mixtures increase with an increasing sterol concentration and are essentially identical but differ in the concentration at which the $L_{\beta'}$ to $P_{\beta'}$ phase transition is

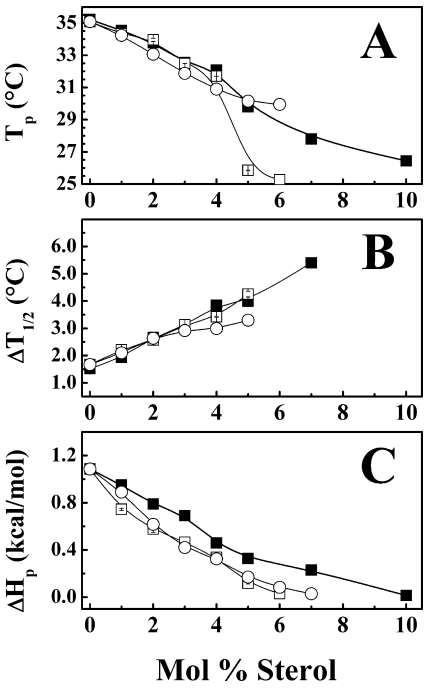


**Figure 4.** Effect of increases in sterol concentration on the $T_p$, $\Delta T_{1/2}$, and $\Delta H_p$ of the pretransition of DPPC: cholesterol/DPPC (■), lathosterol/DPPC (□), and cholestanol/DPPC (○) mixtures. The error bars were typically equal to, or smaller than, the size of the symbols.

abolished, as is seen for the respective $T_p$ and $\Delta H_p$ values. This observation indicates that at very low sterol concentrations, both sterols similarly broaden the DPPC pretransition, despite differences in the double bond position of ring B.

The $\Delta H_p$ values of the Lath/DPPC mixtures follow a decreasing curve with an increasing sterol concentration at a rate slightly greater than those of the Chol-containing DPPC bilayers. At the same sterol concentrations, the $\Delta H_p$ values of the Chol/DPPC mixtures are significantly greater than those of the Lath/DPPC mixtures (Figure 4C). The pretransition enthalpy is close to 0 kcal/mol at a Lath concentration of ~6 mol %, whereas $\Delta H_p$ persists up to a concentration of ~10 mol % in the Chol/DPPC mixtures. Thus, we can conclude that Lath more effectively abolishes the DPPC pretransition than does Chol on a molar basis.

**Effects of Lathosterol on the Main Phase Transition of DPPC.** The DSC data shown in Figure 2 indicate that at low to moderate (≤20 mol %) sterol concentrations, both Lath- and Chol-containing DPPC bilayers exhibit asymmetric thermograms that can be deconvolved into two overlapping, symmetrical thermal events (Figure 5). One of these components is considerably sharper than the other; its peak temperature and cooperativity decrease slightly, and its enthalpy decreases markedly with increasing sterol content. The other component is considerably broader; its midpoint temperature exhibits a more complex dependence on sterol structure and content, and it is the only component persisting at the higher range of sterol concentrations. This pattern of sterol concentration-dependent behavior has been observed previously,[46−50,57−62] and the resolved sharp and broad components have been ascribed to the differential melting of sterol-poor and sterol-rich lipid domains, respectively. However, there are significant differences between the sterol


dx.doi.org/10.1021/bi200721j | *Biochemistry* 2011, 50, 9982−9997

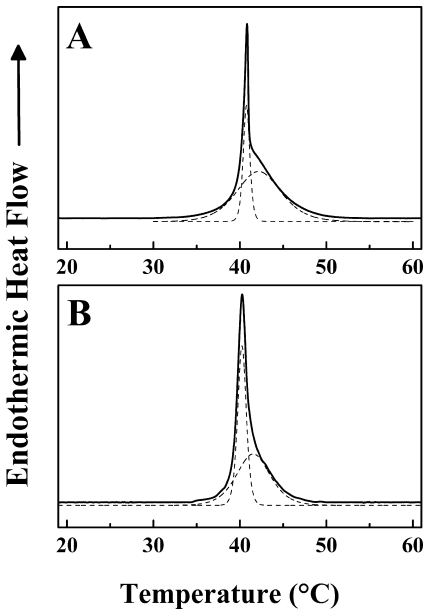


**Figure 5.** Illustration of the results typically obtained in our peak-fitting deconvolution analyses of the DSC thermograms exhibited by cholesterol-containing (A) and lathosterol-containing (B) DPPC bilayers. Both thermograms are from samples containing 15 mol % sterol and were acquired at a scan rate of 10 °C/h. To facilitate visibility, the fitted curves are slightly displaced along the *y*-axis.

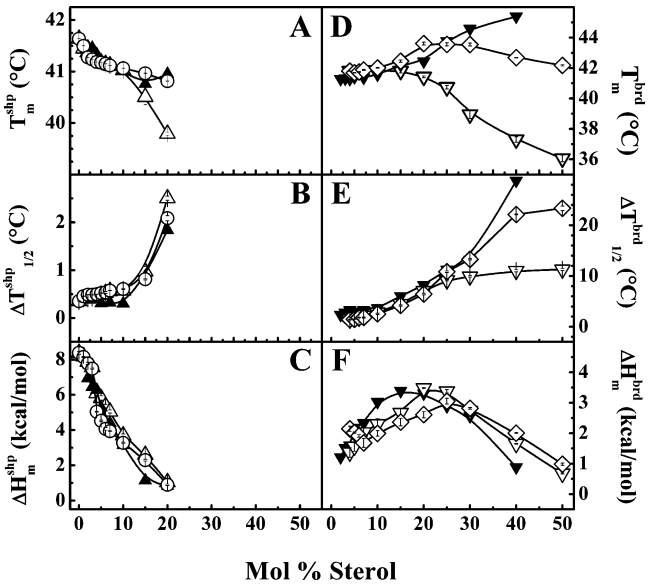


**Figure 6.** Thermodynamic parameters for the deconvolved sharp (A–C) and broad (D–F) components obtained from the DSC heating thermograms of the cholesterol/DPPC (▲ and ▼), lathosterol/DPPC (△ and ▽), and cholestanol/DPPC (○ and ◇) samples as a function of sterol concentration, acquired at scan rate of 10 °C/h. The error bars were typically equal to or smaller than the size of the symbols.

concentration-dependent behaviors exhibited by the Lath- and Chol-containing preparations, especially with regard to the quantitative aspects of the sterol concentration dependence of the overall properties of the underlying sharp and broad peaks. This aspect of our experimental observations was further examined through the application of computer-assisted curve- and peak-fitting procedures to deconvolve the observed DSC thermograms into their component peaks (Figure 5), so that the sterol concentration dependence of each component could be examined and compared (Figure 6).

*Effects of Lathosterol on the Sharp Component of the Main Phase Transition of Sterol/DPPC Mixtures.* The $T_m$ values obtained from the sharp and broad components (distinguished by the superscripts shp and brd, respectively, hereafter) of the main phase transition of both the Lath/DPPC and Chol/DPPC mixtures are shown in Figure 6. The thermodynamic parameters calculated from our DSC heating thermograms for DPPC/sterol mixtures containing 3–10 mol % Lath and Chol have very similar values of $T_m^{shp}$, $\Delta T_{1/2}^{shp}$, and $\Delta H_m^{shp}$ (Figure 6A–C). Corresponding values for cholestanol (5$\alpha$-cholestan-3$\beta$-ol)/DPPC mixtures are identical to those containing Chol.[46,49] All three sterols show a gradual decrease in their $T_m^{shp}$ values, and they are identical within experimental error (Figure 6A). This indicates that they destabilize the gel phase in a similar manner at low sterol concentrations in the sterol-poor domain, regardless of the presence or position of the double bond in ring B. Above 10 mol %, the $T_m^{shp}$ values of the Chol and cholestanol/DPPC mixtures level off, whereas those of Lath/DPPC samples continue to decrease with an increasing sterol concentration. This indicates that further Lath incorporation decreases the stability of the sterol-poor DPPC gel phase domains relative to the liquid-crystalline phase domains more markedly than the incorporation of Chol or cholestanol at sterol concentrations of up to 20 mol %.

The $\Delta T_{1/2}^{shp}$ values (Figure 6B) are inversely related to the cooperativity of the chain-melting phase transition of DPPC in the sterol-poor domains. The corresponding values of $\Delta T_{1/2}^{shp}$ of both sterol/DPPC mixtures (Figure 6B) show little increase up to a concentration of ~7 mol %. At higher sterol concentrations, the $\Delta T_{1/2}^{shp}$ values of Lath/DPPC, Chol/DPPC, and cholestanol/DPPC mixtures increase significantly above 10 mol %, with the Lath-containing mixtures showing a slightly greater increase with an increasing sterol concentration, indicating that Lath has a somewhat greater ability to broaden the DPPC main phase transition in the sterol-poor domains than either Chol or cholestanol.

The $\Delta H_m^{shp}$ values of the three sterol/DPPC systems generally follow a similar decreasing trend with an increasing sterol concentration. At very low concentrations, $\Delta H_m^{shp}$ values for all three sterol/DPPC mixtures are identical within experimental error. However, the $\Delta H_m^{shp}$ values of the Chol/DPPC mixtures from 4 to 15 mol % are lower than those of mixtures containing Lath (Figure 6C). Corresponding $\Delta H_m^{shp}$ values for cholestanol-containing DPPC mixtures are initially lower than those containing either Chol or Lath over the range from 4 to 7 mol % sterol, but above 10 mol % sterol, the $\Delta H_m^{shp}$ values of the cholestanol/DPPC mixtures are higher than those of mixtures containing Chol and converge with the values obtained for the Lath/DPPC mixtures. Although there are minor variations in the decrease in the $\Delta H_m^{shp}$ values with an increasing sterol concentration, the sharp component of the DSC endotherm for each sterol/DPPC mixture is abolished entirely at sterol concentrations above 20 mol %. This observation suggests that these three sterols eliminate the chain-melting phase transition of the sterol-poor domains of DPPC to a similar extent despite the different double bond positions or the absence of a double bond in the polycyclic ring system.


dx.doi.org/10.1021/bi200721j | *Biochemistry* 2011, 50, 9982–9997

*Effects of Lathosterol on the Broad Component of the DPPC Main Phase Transition.* An analysis of the broad components obtained from our deconvolution of the overall DSC heating thermograms for all three sterol/DPPC systems is shown in Figure 6D–F. All three thermodynamic parameters, $T_m^{brd}$, $\Delta T_{1/2}^{brd}$, and $\Delta H_m^{brd}$, show very significant differences among the Lath-, Chol-, and cholestanol-containing DPPC mixtures over the entire concentration range. Specifically, although below 10 mol % sterol the $T_m^{brd}$ values of DPPC mixtures containing the three structurally related sterols superimpose, they gradually diverge with an increasing sterol concentration. Between 10 and 20 mol % sterol, the $T_m^{brd}$ values for the Chol/DPPC and cholestanol/DPPC mixtures continue to increase, whereas that of the Lath-containing mixtures decreases. However, at ~20 mol % sterol, there is an inflection point in the $T_m^{brd}$ values of both the Lath/DPPC and cholestanol/DPPC mixtures, above which they both decline, whereas the $T_m^{brd}$ values for mixtures containing Chol continue to increase with an increasing sterol concentration. The decrease in the $T_m^{brd}$ values of the cholestanol/DPPC mixtures is small and very gradual, whereas the decline in the corresponding values for the Lath-containing mixtures is significantly greater (Figure 6D). These results indicate that at sterol concentrations above 20 mol %, Chol stabilizes whereas Lath and cholestanol destabilize the lower-temperature, sterol-rich domains to different extents.

For each sterol/DPPC system, the $\Delta T_{1/2}^{brd}$ values (Figure 6E) initially show a gradual increase with an increasing sterol concentration up to 25 mol % sterol. Above that concentration, the $\Delta T_{1/2}^{brd}$ values of the Chol/DPPC and cholestanol/DPPC systems continue to increase at all concentrations at which a broad peak remains visible, and thus, the cooperativity of the "gel to liquid-crystalline" phase transition in the sterol-rich domain decreases more rapidly at sterol concentrations above 25 mol % for cholestanol-containing and especially for Chol-containing mixtures. In contrast, above the same concentration, the $\Delta T_{1/2}^{brd}$ values of the Lath/DPPC mixtures increase by only a small amount. This indicates that at higher sterol concentrations, Lath, unlike Chol and cholestanol, is not decreasing the phase transition cooperativity of the sterol-rich domains, and thus, additional Lath molecules are probably not interacting with all of the DPPC molecules present in the binary mixture, probably because of limited lateral miscibility.

The values of $\Delta H_m^{brd}$, which show the ability of the sterol to abolish the chain-melting phase transition of DPPC in the sterol-rich domain, are shown in Figure 6F. The curves for Chol- and for Lath-rich DPPC mixtures are generally similar but show distinct differences (Figure 6F). At lower sterol concentrations, the broad component is observed in DPPC mixtures containing either Chol or Lath starting at ~3 mol % sterol. However, with an increasing sterol concentration, the Chol/DPPC $\Delta H_m^{brd}$ values increase sharply, whereas those of the corresponding Lath-containing DPPC mixtures show a more gradual increase. DPPC mixtures containing Chol reach a maximum $\Delta H_m^{brd}$ value ($\Delta H_m^{brd\text{-}max}$), which may correspond to a miscibility transition,[37,63] at approximately 17 mol % sterol, whereas the corresponding maxima for the Lath- and cholestanol-containing DPPC mixtures occur at 20 and 25 mol % sterol, respectively. Nevertheless, the magnitude of $\Delta H_m^{brd\text{-}max}$ is ~3.5 kcal/mol for all three sterol/DPPC mixtures. Further addition of Lath or Chol results in a gradual reduction in the $\Delta H_m^{brd}$ values in both sterol/DPPC mixtures. DPPC mixtures containing Chol abolish the chain-melting phase transition of DPPC by 50 mol % sterol, whereas similar mixtures containing Lath still show a small endothermic transition whose enthalpy lies at ~0.75 kcal/mol of DPPC at 50 mol % sterol. A closer examination of the leading and trailing edges of the $\Delta H_m^{brd}$ values shows that those obtained for Lath/DPPC and cholestanol/DPPC mixtures more effectively abolish the DPPC chain-melting phase transition compared to corresponding mixtures containing Chol at lower sterol concentrations. Thus, Chol more effectively abolishes the melting of the DPPC acyl chains than does Lath or cholestanol at higher, physiologically relevant sterol concentrations.

The inability of Lath and cholestanol to abolish the chain-melting phase transition of DPPC at the same concentrations used in our Chol/DPPC mixtures is also evident in the plot of the total main phase transition enthalpy versus sterol concentration shown in Figure 7. This figure illustrates that

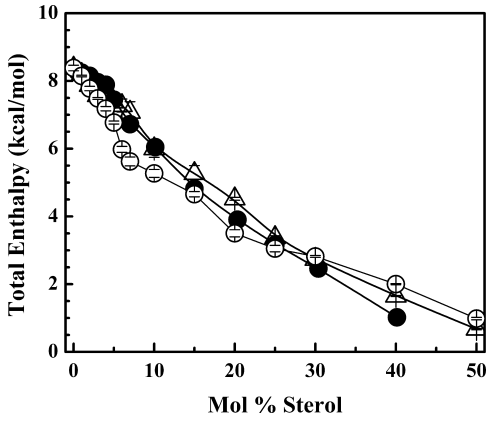


**Figure 7.** Overall enthalpy values obtained for Chol/DPPC (●), Lath/DPPC (△), and cholestanol/DPPC (○) mixtures from DSC heating curves. The error bars were typically equal to or smaller than the size of the symbols.

the rate of decrease of the total enthalpy of the chain-melting phase transition is lower for Lath/DPPC and cholestanol/DPPC mixtures than for Chol/DPPC mixtures at higher sterol concentrations, and that a phase transition still persists for the former two sterols, but not for the latter, at 50 mol % sterol. These results support the idea that Lath (and, to a lesser degree, cholestanol) has a lower lateral miscibility in DPPC bilayers than Chol does. This interpretation is consistent with recent studies of sterol/PC monolayers, which show that Chol is fully miscible with DPPC, forming a continuum over the range of 0–50 mol %.[37] In contrast, sterols that are structurally different from Chol are only partially miscible in DPPC and exhibit discrete regional stoichiometries.

**Fourier Transform Infrared Spectroscopic Studies of the Thermotropic Phase Behavior and Organization of Lathosterol/DPPC Mixtures.** Illustrated in Figure 8 are some of the temperature-induced changes in the FTIR spectra exhibited by a 30 mol % Lath/DPPC mixture over the temperature range of 0–60 °C. The data shown exhibit several features shared by all of the sterol-free and sterol-containing DPPC bilayers studied here. The dominant features of the C–H stretching region (3000–2800 $cm^{-1}$) are absorption bands centered near 2849–2852 and 2916–2922 $cm^{-1}$. These bands arise from the symmetric and asymmetric C–H stretching vibrations of the methylene groups on the hydrocarbon chains and are sensitive to the conformational order of the

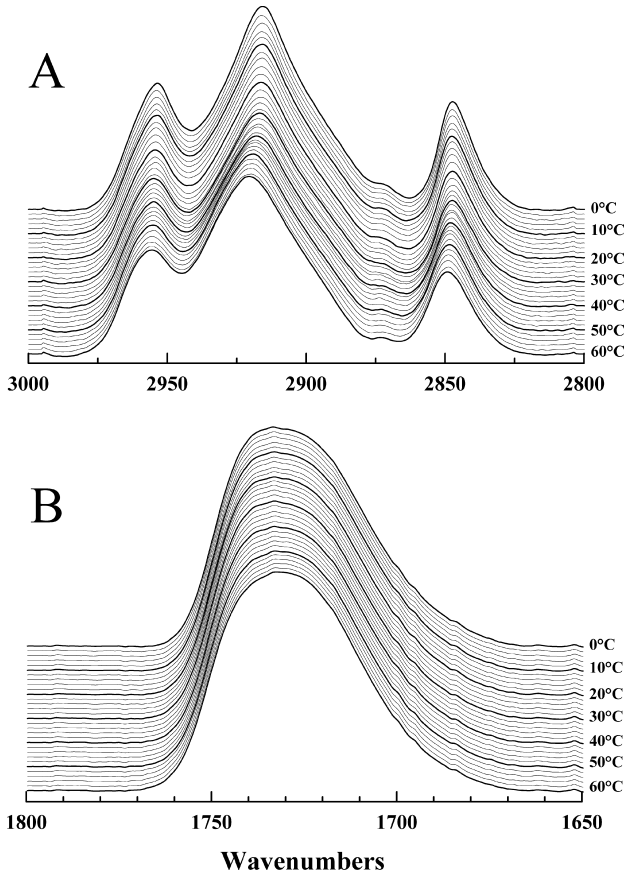


**Figure 8.** Stacked plots illustrating some of the temperature-induced changes in the FTIR spectra exhibited by a sample of 30 mol % Lath/DPPC model membranes. The absorbances shown were acquired at the indicated temperatures and illustrate the changes observed in the contours of the C−H stretching (A) and C═O stretching (B) absorption bands of the sample.

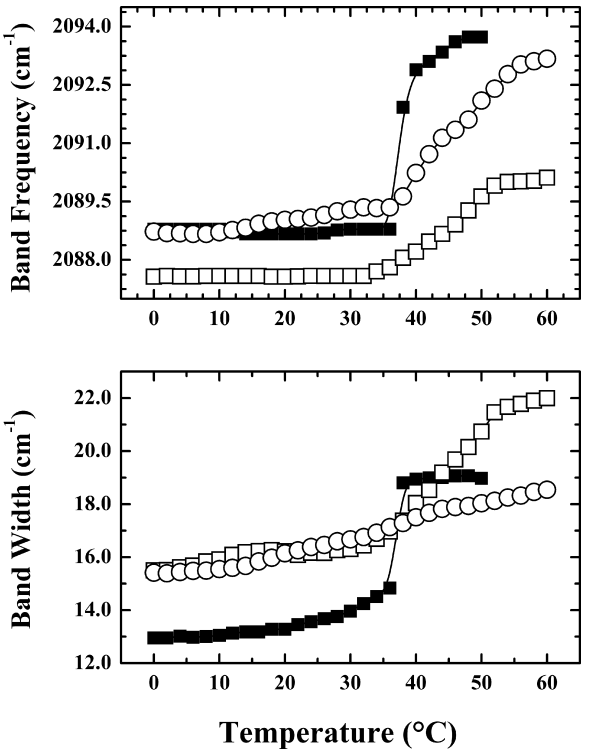


**Figure 9.** Temperature-dependent changes in the properties of the C−D stretching band exhibited by sterol-free DPPC-$d_{62}$ bilayers (■) and by DPPC-$d_{62}$ bilayers containing ∼30 mol % Chol (□) and ∼30 mol % Lath (○). The data shown were obtained by analyses of spectra acquired in the heating mode, with the top panel illustrating the temperature-induced changes in the band maxima and the bottom panel showing the corresponding changes in overall bandwidth.

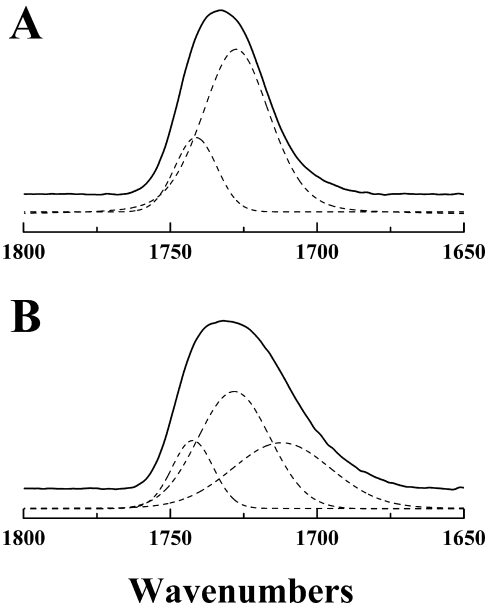


**Figure 10.** Component structure of the ester carbonyl absorption bands exhibited by sterol-free (A) and Lath-rich (B) DPPC-$d_{62}$ bilayers. The absorbance spectra shown were acquired at 6 °C with the solid lines indicating the observed baseline-subtracted absorption band envelopes and the dashed lines indicating estimates of the properties of the component bands.

hydrocarbon chains (i.e., the relative number of *trans* and *gauche* rotational conformers present in these chains). At temperatures below the onset of the hydrocarbon chain-melting phase transition, these vibrational modes give rise to sharp absorption peaks centered near 2849 and 2916 $cm^{-1}$, respectively. At the main chain-melting phase transition, there is a discontinuous increase in the frequency (2−5 $cm^{-1}$) and width (∼15%) of these absorption bands. The combination of these changes reflects the increase in the *gauche* rotamer content and mobility of the lipid hydrocarbon chains, respectively, and is typically used as an IR spectroscopic marker of hydrocarbon chain-melting phase transitions (see refs 54 and 64−66). The gel to liquid-crystalline phase transitions of samples prepared from chain-perdeuterated phospholipids are also accompanied by changes in the frequencies and widths of the $CD_2$ stretching bands (Figure 9). However, because of the greater reduced mass of the $CD_2$ group, those absorption bands are observed at frequencies between 2050 and 2250 $cm^{-1}$.

In the 1650−1800 $cm^{-1}$ region (Figures 8B and 10), the broad absorption band centered near 1740 $cm^{-1}$ arises from the C═O stretching vibrations of the ester carbonyl groups at the bilayer polar−apolar interfacial region. As with most fully hydrated glycerolipid bilayers, this band can be resolved into components that have been assigned to populations of "free" and H-bonded ester carbonyl groups (refs 54 and 64−66 and references cited therein), whose relative integrated intensities usually change at the gel to liquid-crystalline phase transition.


dx.doi.org/10.1021/bi200721j | *Biochemistry* 2011, 50, 9982−9997

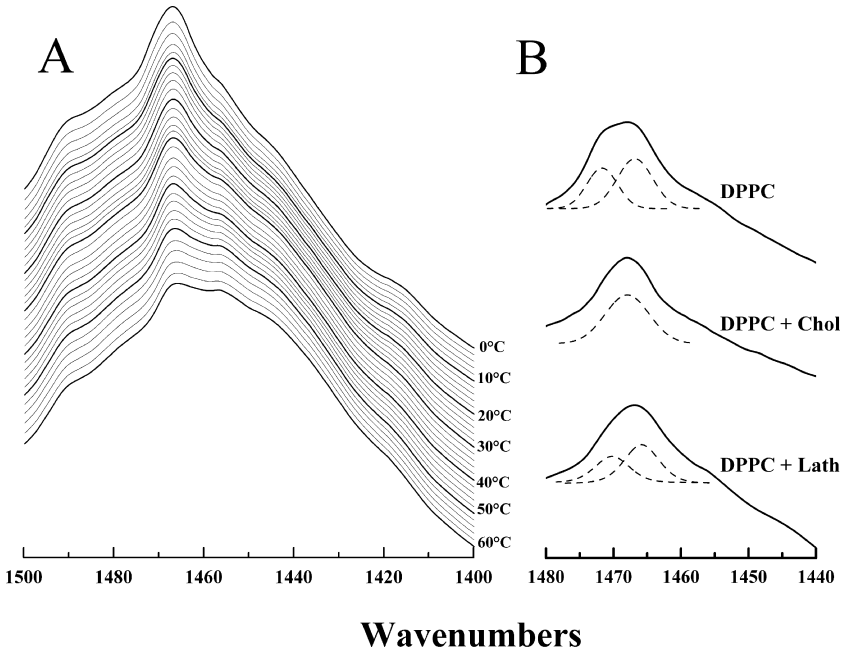


**Figure 11.** Absorbance spectra illustrating the effect of Lath and Chol on the contours of the $CH_2$ scissoring bands of DPPC. Panel A is a stacked plot showing the temperature-induced changes in the scissoring bands exhibited by a 30 mol % Lath/DPPC mixture. Panel B shows the low-temperature factor group splitting of the $CH_2$ scissoring bands exhibited by the sterol-free, Chol-rich, and Lath-rich DPPC model membranes. The spectra shown in the right panel were acquired at 2 °C with the solid lines indicating the observed bands and the dashed lines indicating our estimates of the shape and relative intensities of the underlying components.

For example, with DPPC bilayers, the C═O stretching band can be resolved into components centered near 1728 $cm^{-1}$ (H-bonded) and 1743 $cm^{-1}$ (non-H-bonded), and at the main chain-melting phase transition, there is an increase in the relative contribution of the H-bonded population. Because water is the predominant source of H-bonding donor groups in those bilayers, this observation is usually interpreted in terms of phase-state-induced changes in hydration of and H-bonding interactions in the polar/apolar interfacial regions of those bilayers.

Finally, the main feature of the C−H deformation region between 1500 and 1400 $cm^{-1}$ is an absorption band centered near 1465−1472 $cm^{-1}$ (Figure 11A), which arises from the methylene scissoring vibrations. This band is sensitive to the lateral-packing interactions between adjacent hydrocarbon chains. Thus, it provides information about the nature of the hydrocarbon chain packing existing within the lipid bilayer, particularly at lower temperatures where these chains exist in an all-*trans* conformation. The relative effects of the incorporation of 30 mol % Lath or Chol into DPPC bilayers on the thermally induced changes in these three regions of the IR spectrum are examined in detail below and correlated with the calorimetrically resolved thermotropic phase changes described above.

*$CD_2$ Stretching Absorption Bands.* Figure 9 shows a comparison of the temperature-induced changes in the frequencies and bandwidths of the $CD_2$ symmetric stretching bands exhibited by sterol-free DPPC-$d_{62}$ bilayers and by DPPC-$d_{62}$ bilayers containing either 30 mol % Chol or Lath. The frequency and bandwidth of the $CD_2$ symmetric stretching bands of pure DPPC bilayers increase sharply at temperatures centered near 38 °C, consistent with the occurrence of a highly cooperative hydrocarbon chain-melting phase transition at that temperature. In contrast, the corresponding temperature-induced changes in the frequency of the $CD_2$ symmetric stretching band exhibited by the Chol- and Lath-containing DPPC bilayers span a considerably broader temperature range, consistent with the broader hydrocarbon chain-melting phase transitions exhibited by the sterol-containing samples examined by DSC (Figure 2). A similar pattern was also observed in plots of the $CH_2$ symmetric stretching bands exhibited by the corresponding sterol-free and sterol-containing DPPC samples, although the temperature ranges of those changes are shifted upward by some 3−4 °C, as expected (data not shown). The nature of the changes occurring with the Chol-containing sample was described fully in previous publications from this laboratory[59,62] and will not be examined in detail here. Note that the curve describing the changes in the $CD_2$ symmetric stretching frequency of the Lath-containing sample is centered at a lower temperature and spans a broader temperature range and $CD_2$ frequency range than that of the Chol-containing DPPC mixture, consistent with the broader and more enthalpic phase transition observed calorimetrically. Moreover, the onset and completion temperature and the midpoint temperature of the FTIR spectroscopic and DSC curves coincide closely, considering that the $T_m$ of the DPPC-$d_{62}$ used in FTIR spectroscopic experiments is lower than that of the non-perdeuterated DPPC used in the DSC experiment. These results indicate that the broad endothermic component observed by calorimetry arises from a gradual hydrocarbon chain-melting phase transition of the host DPPC bilayer from a gel-like to fluid-like phase. Moreover, the higher $CD_2$ frequencies observed at both low and high temperatures in the Lath-containing, as opposed to Chol-containing, mixtures suggest that the presence of Lath does not conformationally order the DPPC hydrocarbon chains to the same extent as the presence of an equal amount of Chol.

*Carbonyl Stretching Absorption Bands.* As illustrated in Figure 10 (top panel), the ester C═O stretching bands


dx.doi.org/10.1021/bi200721j | *Biochemistry* 2011, 50, 9982−9997

exhibited by sterol-free DPPC bilayers consist of a broad envelope comprising two subcomponents centered near 1728 and 1743 $cm^{-1}$. Previous studies from this laboratory have also shown that similar components are present in Chol-containing DPPC bilayers, although the relative integrated intensities of these components differ from those present in the sterol-free DPPC bilayers.[46,47] Figure 10 also shows the results of a typical component analysis of ester carbonyl stretching bands of a 30 mol % Lath/DPPC sample. Our analyses indicate that the ester carbonyl stretching bands of the Lath-containing sample consist of a summation of three components centered near 1711, 1728, and 1743 $cm^{-1}$. The presence of the additional low-frequency ester carbonyl subcomponent near 1710 $cm^{-1}$ indicates that Lath-rich DPPC bilayers contain a population of H-bonded ester carbonyl groups that is absent from or negligibly small in both the sterol-free and Chol-containing DPPC bilayers. The bandwidth of this low-frequency component is relatively large, suggesting that there is considerable heterogeneity in the local environment of the ester C═O groups concerned. Our analyses of the component structure of the C═O stretching band envelope also indicate that the contribution of this band to the integrated intensity of the ester C═O bands is essentially constant over the entire temperature range studied, and that temperature- and/or phase-state-dependent changes in the relative integrated intensities of the other two bands are considerably smaller than those typical of the corresponding sterol-free and Chol-rich DPPC bilayers (see Table 1). Thus, it appears that the three-component structure of the ester carbonyl absorption bands of Lath-rich DPPC bilayers is relatively insensitive to the temperature and/or the phase state of the bilayer, behavior that is atypical of the sterol-containing DPPC bilayers examined so far (for examples, see refs 46, 47, and 67). The probable basis of the appearance of the additional lower-frequency population of ester carbonyl groups, and of the seemingly anomalous temperature and phase-state dependence of the ester carbonyl absorption bands of the Lath/DPPC samples, will be explored in Discussion.

**Table 1. Characterization of the Subcomponents of the Ester C═O Stretching Bands Exhibited by Hydrated, Sterol-Free, and Sterol-Containing DPPC Bilayers**[a]

| peak maximum ($cm^{-1}$) | peak width ($cm^{-1}$) | peak area (% of the total) |
|---|---|---|
| (A) DPPC and 30 mol % Lathosterol (solid-disordered phase at 6 °C) | | |
| 1711 | 37 | 33.6 |
| 1727 | 27 | 44.6 |
| 1743 | 18 | 21.8 |
| (B) DPPC and 30 mol % Lathosterol (liquid-ordered phase at 60 °C) | | |
| 1711 | 37 | 33.6 |
| 1729 | 28 | 48.4 |
| 1743 | 18 | 18.0 |
| (C) DPPC ($L_\beta$ phase at 6 °C) | | |
| 1726 | 27 | 76 |
| 1740 | 17 | 24 |
| (D) DPPC ($L_\alpha$ phase at 60 °C) | | |
| 1727 | 31 | 82 |
| 1741 | 18 | 18 |
| (E) DPPC and 30 mol % Cholesterol (solid-disordered phase at 6 °C) | | |
| 1722 | 36 | 80 |
| 1740 | 18 | 20 |
| (F) DPPC and 30 mol % Cholesterol (liquid-ordered phase at 60 °C) | | |
| 1721 | 39 | 84 |
| 1741 | 21 | 16 |

[a]Parameter values are all rounded to the nearest whole number. Phase nomenclature follows that of McMullen et al.[11]

*$CH_2$ Scissoring Absorption Bands.* The left panel in Figure 11 shows a stacked plot illustrating the temperature-dependent changes in the contours of the $CH_2$ scissoring bands arising from hydrocarbon chain methylene groups in a sample of 30 mol % sterol Lath/DPPC bilayers. At low temperatures, the main absorption band near 1465 $cm^{-1}$ consists of a relatively broad asymmetric band envelope that can be resolved into components centered near 1472 and 1466 $cm^{-1}$. This observation is a manifestation of the so-called factor group splitting of the $CH_2$ scissoring band, the result of interchain coupling of the scissoring vibrations of methylene groups on all-*trans* polymethylene chains packed in an orthorhombic perpendicular subcell (refs 54, 64, and 66 and references cited therein). Its occurrence in the low-temperature FTIR spectra of the Lath-containing sample indicates that the DPPC/Lath bilayers contain extended arrays of closely packed all-*trans* DPPC hydrocarbon chains at low temperatures. Upon heating, the magnitude of the factor group splitting gradually diminishes and effectively collapses at temperatures near 20 °C, such that a single symmetrical band is observed at frequencies near 1467 $cm^{-1}$. When the sample is further heated to temperatures near and above the hydrocarbon chain-melting phase transition temperature of the sample, this band broadens considerably. The latter spectroscopic changes are observed with the sterol-free and sterol-containing preparations and are consistent with the increased mobility of the methylene groups that occurs at lipid hydrocarbon chain-melting phase transitions. However, the thermally induced collapse of factor group splitting observed at temperatures well below the onset of the hydrocarbon chain-melting phase transition is of special significance to this work, because it is indicative of a thermally induced weakening of lateral interactions between hydrocarbon chains. In hydrocarbon chain-homogeneous systems (e.g., pure DPPC), that process is entirely attributable to thermally induced increases in the rates and amplitudes of the reorientational fluctuations of the hydrocarbon chains. However, with the sterol-containing bilayers, there are also other potential contributory factors, the nature and significance of which will be examined later. However, our data also show that the low-temperature factor-group splitting is not discernible with the Chol-containing system, and that it is more pronounced in pure DPPC bilayers than in the Lath-rich mixtures (Figure 11B). These observations indicate that the incorporation of ~30 mol % Chol into DPPC bilayers completely inhibits the formation of extended domains of laterally interacting, all-*trans* hydrocarbon chains at low temperatures, whereas the presence of Lath only partially inhibits their formation. Given this and the fact that the formation of sterol-poor DPPC domains within sterol-rich DPPC bilayers requires some degree of sterol/DPPC demixing, it follows that the DPPC/Lath mixture must be more prone to low temperature-induced demixing than the corresponding Chol/DPPC mixture. This suggestion has important implications regarding the relative miscibilities of Chol and Lath in DPPC bilayers, which will be explored in Discussion.

## DISCUSSION

In this comparison of the thermotropic phase behavior of two sterol/DPPC mixtures, we also note that both Lath and Chol have planar ring systems but differ in having a double bond at

$\Delta^5$ (Chol)[46] or $\Delta^7$ (Lath). We also recently reported a comparative study of the epimeric 3-cholestanols, which have no double bond in the steroid nucleus but have a 5α-H configuration like that of Lath.[49] These three sterols also all have the same alkyl side chain structure and similar calculated cross-sectional areas. This implies that the majority of changes in the thermodynamic parameters of the pretransition and main transition of DPPC can be reasonably attributed to differences in the ring B configuration of the respective sterols and, consequently, their effect on the nature and stoichiometry of sterol−DPPC interactions and the resulting packing of both molecules in the bilayer membrane.

Our earlier studies of the comparative effects of the incorporation of Chol and other sterols on the pretransition of DPPC also demonstrated that this phase transition persisted to approximately 10 mol % sterol in the case of Chol, but only to ∼8, ∼7, and ∼6 mol % in the case of lanosterol,[46] epicholesterol,[47] and ergosterol,[48] respectively. We rationalized these results as follows, largely on the basis of the relative cross-sectional areas of Chol and the other three sterols. Because Chol has a small cross-sectional area, we reasoned that the incorporation of a greater amount of Chol would be required to abolish the hydrocarbon chain tilt in the $L_\beta'$ and $P_\beta'$ phases of DPPC to provide a match between the smaller cross-sectional areas of the saturated hydrocarbon chains relative to the larger cross-sectional area of the DPPC polar headgroup in the gel phase, as Chol itself has a very small polar headgroup. Thus, the larger cross-sectional area of Lan, Erg, and Echol molecules would make the latter sterols capable of relieving this mismatch in the cross-sectional area of the DPPC hydrocarbon chains and polar headgroups at progressively lower sterol concentrations. We also pointed out that each of these sterols caused more disorder in the DPPC gel state than Chol, which would further expand the area of the DPPC hydrocarbon chains, augmenting the effects due to differences in the intrinsic cross-sectional area of these sterols. Although this explanation still seems reasonable to us, these results with Lath/DPPC mixtures, and our recently published results with comparable cholestanol/DPPC mixtures,[49] would not be expected on the basis of this reasoning, because although both sterols have cross-sectional areas similar to that of Chol, they nevertheless still abolish the pretransition at sterol concentrations of only ∼6−7 mol %. Moreover, our unpublished FTIR results do not indicate that cholestanol disorders the hydrocarbon chains in gel-state DPPC bilayers to a greater extent than Chol. Thus, our results do not in fact support the idea that the effects of various sterols on the pretransition of PC bilayers are exclusively or even primarily determined by their relative cross-sectional areas. Therefore, there must be another molecular explanation for these results, such as differences in sterol tilt angles and/or the number and strength of sterol−water−PC H-bonds in the polar headgroup and interfacial regions.[68−70] The resolution of these issues will require additional X-ray diffraction and other studies to determine the underlying molecular mechanism. However, we can conclude from our data that the difference in the position of the double bond in ring B of Lath and Chol produces a clear difference in their abilities to abolish the pretransition of DPPC, even to the extent that the presence of a double bond at C7 of Lath has the same effect as its complete removal, as in cholestanol. However, the presence of the $\Delta^7$ double bond in Lath does produce a biphasic dependence of the $T_p$ on sterol concentration, an effect not seen previously in our studies of Chol/DPPC mixtures or those containing any other sterol.

The $\Delta T_{1/2}^{brd}$ values of Lath- and Chol-containing DPPC mixtures (Figure 6E) show that both sterols broaden the chain-melting phase transition of the sterol-rich domain of the DPPC bilayer in a similar fashion up to ∼25 mol % sterol. If Chol is more miscible than Lath at higher sterol concentrations in the DPPC bilayer, the peak half-width of the Chol/DPPC endotherm should be significantly greater than that of Lath-containing DPPC mixtures. Figure 6E clearly shows that above 25 mol % sterol, Chol continues to broaden the chain-melting phase transition significantly, whereas the corresponding $\Delta T_{1/2}^{brd}$ values obtained for the Lath/DPPC mixtures plateau above 30 mol % sterol. This suggests that Lath less effectively perturbs the melting of the DPPC acyl chains with an increasing sterol concentration and that it may be approaching its miscibility limit in the sterol-rich DPPC bilayer above 30 mol % sterol.[63,70] Our FTIR measurements of 30 mol % Lath/DPPC-$d_{62}$ samples obtained at lower temperatures certainly suggest that Lath is intrinsically less miscible than Chol in the sterol-rich DPPC domain, as has previously been suggested on the basis of monolayer measurements.[37,40] However, a simple miscibility limit above 30 mol % Lath is not consistent with the decreasing values of $\Delta H_m^{brd}$ above 30 mol % sterol observed here (Figure 6F), indicating that Lath continues to be incorporated to a reduced degree into the DPPC bilayer, but not to the extent that the DPPC chain-melting phase transition is abolished entirely at 50 mol %. This result also suggests a more complex interpretation is necessary in this case (see below).

Corresponding $\Delta T_{1/2}^{brd}$ values of cholestanol/DPPC mixtures[49] above 30 mol % sterol are intermediate between those of Chol and Lath (Figure 6E), suggesting that the bilayer can accommodate the saturated sterol at high concentrations, although it is not as fully miscible as Chol in Chol/DPPC mixtures, in agreement with both monolayer film and fluorescence microscopy studies, which have shown that the cholestanol/DPPC mixtures have molecular areas similar to but collapse pressures significantly lower than those of Lath- or Chol-containing DPPC mixtures.[37,71] More recent measurements over a wide range of pressures show that the cholestanol has a slightly smaller molecular area, but a greater deviation from packing ideality, than Chol or Lath,[72] indicating significant differences in the relative proportion of interactions between like and unlike pairs.[73] The sterol miscibility in the DPPC bilayer with an increasing concentration determines the extent of laterally segregated liquid-ordered domains in the sterol/DPPC mixture.[37,43,70,74]

It is also interesting that corresponding values of $\Delta T_{1/2}^{shp}$ and $\Delta T_{1/2}^{brd}$ (Figure 6B,E) follow a different incremental order in each panel at higher sterol concentrations in the respective sterol-rich domains. In the sterol-poor domain, Lath is slightly more effective than Chol in broadening the DPPC gel to liquid-crystalline phase transition, whereas in the sterol-rich domain above 30 mol % sterol, Chol more effectively broadens the DPPC chain-melting phase transition than does Lath. A comparison with the $\Delta T_{1/2}$ values for the corresponding cholestanol/DPPC mixtures[49] reveals that the different incremental order (unlike the corresponding $T_m^{shp/brd}$ values) is the result of a significant change in the ability of Chol to broaden the phase transition of DPPC bilayers and the relative proportions of more ordered and less ordered sterol-rich domains relative to those of Lath/DPPC and cholestanol/DPPC mixtures. This most likely signifies a difference in the miscibility of Lath and Chol in the sterol-enriched more

ordered versus the less ordered phases of DPPC, reflecting differences in the balance of favorable sterol−lipid interactions in Lath/DPPC and Chol/DPPC bilayers, arising from their different chemical configurations. These interactions have several potential consequences for the sterol/lipid bilayer properties, which we will discuss below.

To ascertain the underlying nature of the molecular contributions determining the physical properties of DPPC mixtures containing either Lath or Chol, we must examine our present DSC and FTIR results in a broader context. Our FTIR analyses of the ester C═O absorption bands exhibited by the Lath/DPPC mixtures (30 mol %) show a multicomponent band envelope containing components comparable to those observed in the sterol-free and Chol-containing preparations (i.e., ∼1743 and 1728 $cm^{-1}$) and an additional low-frequency component (∼1710 $cm^{-1}$) that is either absent from or negligibly small in both the sterol-free and Chol-containing DPPC bilayers. Comparable behavior have been noted with Erg-rich DPPC bilayers[48] and in fully hydrated PE bilayers,[75] for which the low frequency was attributed to a population of strongly H-bonded ester C═O groups. Although the physical basis of this behavior is unclear, the only sources of H-bonding donor groups in the bilayer interface are water and the Lath hydroxyl group. Moreover, the amount of water available for potential H-bonding interaction with the DPPC carbonyl groups is considerably greater than the amount of sterol present. Therefore, in the presence of an excess of water, considerations of mass action effects alone would suggest that the two populations of H-bonded ester C═O groups are more likely to arise from different populations of water-bonded C═O groups rather than from discrete populations of sterol-bonded and water-bonded ester carbonyl groups. Thus, when compared with the case for the Chol-rich bilayers, the occurrence of this additional population of H-bonded ester carbonyls in the Lath-rich DPPC bilayers could be reflecting differences between the hydration and overall polarity of the bilayer interface arising from the differences between the positions of the sterol ring C═C bond. However, because the total number of H-bonded DPPC carbonyl groups is not greatly different in the Lath/DPPC and Chol/DPPC binary mixtures containing 30 mol % sterol (2.0 and 1.7 carbonyl groups per DPPC molecule, respectively), we cannot rule out a different contribution of sterol hydroxyl and DPPC carbonyl interactions.

The weak temperature dependence in the $CH_2$ scissoring absorption bands in the more ordered $l_o$ phase region of the 30 mol % Lath/DPPC mixture provides evidence of low-temperature sterol−DPPC demixing in the Lath-containing but not in the Chol-containing mixture. Thus, the weak temperature dependence of the C═O stretching and $CH_2$ scissoring bands seen at lower temperatures may arise from the lower miscibility of Lath in the more ordered $l_o$ phase of DPPC and consequently a difference in the miscibility of Lath across the DPPC chain-melting phase transition. This is one possible explanation for the disparate behavior evident in a comparison of the $\Delta T_{1/2}^{brd}$ and $\Delta H_m^{brd}$ values, which show that the $\Delta T_{1/2}^{brd}$ parameter for Chol becomes infinitely broad above 40 mol % whereas that for Lath does not increase above 30 mol % sterol (Figure 6E). However, if Lath is completely immiscible in the DPPC bilayer at higher sterol concentrations, the $\Delta H_m^{brd}$ parameter should not continue to decrease above that concentration, supporting the idea of a mixture of sterol- and DPPC-rich domains differing in their cooperativity being present. Although the $\Delta T_{1/2}^{brd}$ parameter certainly reflects the influence of sterol immiscibility in our studies of epicholestanol/DPPC and epicoprostanol/DPPC mixtures at high sterol concentrations, because the decrease in $\Delta H_m^{brd}$ values is small here,[49,50] $\Delta T_{1/2}^{brd}$ may be reporting a combination of properties in the sterol/lipid bilayer in the case of Lath-rich DPPC bilayers.

Our interpretations raise important questions about a potential molecular mechanism explaining the differences in our DSC and FTIR measurements of Chol- and Lath-containing DPPC mixtures. Although there is a difference in the H-bonding interactions between water and the PC carbonyl groups in the Lath/DPPC and Chol/DPPC bilayers, we cannot eliminate potential contributions to the properties of the sterol-poor and sterol-rich domains of these respective sterol/DPPC systems arising from differences in sterol tilt or from a combination of sterol tilt and interfacial hydration, however defined.[76−79] Our preliminary computer chemistry calculations over a wider range of ring and alkyl side chain conformational space show significant differences in the average vector of the molecular dipole moment above and below the plane of the ring system between Drieding-minimized molecular models of Lath and Chol. It is known that external electric fields can interact with the molecular dipole and, consequently, determine the mean two-dimensional tilt of the molecule about its long axis in condensed monolayer films.[80,81] Similar behavior has been observed in the smectic C phase of liquid crystals,[82,83] and such effects are moderated by the electronic structure of the molecules in the molecular assembly[84,85] and also by the phase structure.[86] Moreover, measurements of pure and mixed lipid films have found a relationship among molecular tilt, dipole density, and domain shape.[87−90] Although the latter reports contain measurements of lipid monolayer films rather than lipid bilayers, they suggest a possible physicochemical mechanism behind the stoichiometric dependence of the thermotropic phase behavior seen in the Lath/DPPC and Chol/DPPC mixtures measured by DSC and FTIR spectroscopy in this study, linking the sterol chemical configuration, conformation, electronic properties, dipole moment, and molecular tilt in the DPPC bilayer, which are consistent with recent molecular modeling calculations of sterol/DPPC bilayers[68,76−79,91−96] and empirical thermodynamic models.[97,98]

The DSC and FTIR measurements described above show that having a double bond in ring B is better than having no double bond at all, but sterols with a $\Delta^5$ double bond are more miscible and better able to abolish the chain-melting phase transition than those with a $\Delta^7$ double bond. This observation has important ramifications when membrane-associated processes are under biophysical rather than under biochemical control. If our interpretations of the results presented here and those in the literature are reasonable, the underlying interactions between sterols and phospholipids may be more complicated than has previously been envisaged.

It has been reported that Chol plays multiple roles in eukaryotic and even in sterol-dependent prokaryotic cells (see ref 24). In addition to its well-known bulk role in regulating the fluidity and order of the lipid bilayer of the plasma membrane, much smaller amounts of Chol are also involved in regulating a number of biochemical and cell biological processes. The former role seems to require any of a series of membrane-active sterols having the same general chemical structure as Chol, but the latter can be quite specific for Chol (or a related sterol). Thus, in certain yeast,[99,100] fungi,[101] or mycoplasma[24] sterol

auxotrophs, a variety of Chol analogues will support cell growth only if supplemented with very small amounts of Chol (or other sterol), which by itself is not capable of supporting growth at such low concentrations. Interestingly, in yeast, the $\Delta^4$ isomer of Chol, by itself, is not able to support growth at such low concentrations. Similarly, several Chol auxotrophic mammalian cell lines do not grow when supplemented with either the cholestanol or the $\Delta^4$ or $\Delta^7$ isomer of Chol.[102] Moreover, the fully saturated Chol analogue cholestanol alone is unable to support the growth of auxotrophic yeast[39] or fungi.[101] However, in the silkworm, although growth was much better with Chol, moderate growth was observed with cholestanol and Lath alone.[103] Taken together, these findings indicate that the presence and position of the double bond in Chol analogues can be crucial in supporting cell growth, if not membrane bilayer fluidity. However, the results presented in this study and others reviewed in the introductory section indicate that the physical properties and interactions of Lath with phospholipid bilayers are sufficiently different from those of Chol that they support the hypothesis that Lath may exert some of its deleterious effects on cell growth and development via a membrane-based biophysical mechanism, in addition to biochemical and regulatory processes.

## AUTHOR INFORMATION


### Corresponding Author

*Telephone: (780) 492-2413. Fax: (780) 492-0886. E-mail: rmcelhan@ualberta.ca.



### Funding

Supported by operating and major equipment grants from the Canadian Institutes of Health Research and by major equipment grants from the Alberta Heritage Foundation for Medical Research. M.G.K.B. was supported by undergraduate Summer Student Research Awards from the Natural Sciences and Engineering Research Council of Canada and by the Alberta Heritage Foundation for Medical Research.


## ABBREVIATIONS

Chol, cholesterol; Lath, lathosterol; Lano, lanosterol; Erg, ergosterol; Echol, epicholesterol; PC, phosphatidylcholine; DPPC, dipalmitoylphosphatidylcholine; DMPC, dimyristoylphosphatidylcholine; DOPC, dioleoylphosphatidylcholine; DOPE, dioleoylphosphatidylethanolamine; PSM, *N*-palmitoylsphingomyelin; PDHSM, *N*-palmitoyldihydrosphingomyelin; DSC, differential scanning calorimetry; FTIR, Fourier transform infrared; NMR, nuclear magnetic resonance; pfg, pulsed-field gradient; POPE, 1-palmitoyl-2-oleoylphosphatidylethanolamine; $T_p$, pretransition temperature maximum; $T_m$, main transition temperature maximum; $\Delta H$, transition enthalpy; $\Delta T_{1/2}$, width of the phase transition at half-height, inversely related to the cooperativity of the phase transition; $L_{\beta'}$ and $L_{\beta}$, lamellar gel phases with tilted and untilted hydrocarbon chains, respectively; $P_{\beta'}$, rippled gel phase with tilted hydrocarbon chains; $L_{\alpha}$, lamellar liquid-crystalline phase; $l_o$, lamellar liquid-ordered phase; $l_d$, lamellar liquid-disordered phase. The superscripts shp and brd appended to the thermodynamic parameters refer to the sharp and broad components of the main phase transition of the sterol-containing DPPC bilayers, respectively.

## REFERENCES


(1) Nes, W. R., and McKean, M. L. (1977) *Biochemistry of Steroids and Other Isopentenoids*, University Park Press, Baltimore.

(2) Yeagle, P. L. (1988) Cholesterol and the cell membrane. In *The Biology of Cholesterol* (Yeagle, P. L., Ed.) CRC Press, Inc., Boca Raton, FL.

(3) Liscum, L., and Munn, N. J. (1999) Intracellular cholesterol transport. *Biochim. Biophys. Acta 1438*, 19−37.

(4) Demel, R. A., and de Kruijff, B. (1976) The function of sterols in membranes. *Biochim. Biophys. Acta 457*, 109−132.

(5) Vist, M. R., and Davis, J. H. (1990) Phase equilibria of cholesterol/DPPC mixtures: $^2$H-nuclear magnetic resonance and differential scanning calorimetry. *Biochemistry 29*, 451−464.

(6) Finegold, L., Ed. (1993) *Cholesterol in Model Membranes*, CRC Press, Inc., Boca Raton, FL.

(7) McMullen, T. P. W., and McElhaney, R. N. (1996) Physical studies of cholesterol-phospholipid interactions. *Curr. Opin. Colloid Interface Sci. 1*, 83−90.

(8) Ipsen, J. H., Karlstrom, G., Mouritsen, O. G., Wennerstrom, H. W., and Zuckermann., M. (1987) Phase equilibria in the phosphatidylcholine-cholesterol system. *Biochim. Biophys. Acta 905*, 162−172.

(9) Thewalt, J. L., and Bloom, M. (1992) Phosphatidylcholine:cholesterol phase diagrams. *Biophys. J. 63*, 1176−1181.

(10) Reinl, H., Brumm, T., and Bayerl, T. M. (1992) Changes in the physical properties of the liquid-ordered phase with temperature in binary mixtures of DPPC with cholesterol: A $^2$H-NMR, FTIR, DSC and neutron scattering study. *Biophys. J. 61*, 1025−1035.

(11) McMullen, T. P. W., and McElhaney, R. N. (1995) New aspects of the interactions of cholesterol and dipalmitoylphosphatidylcholine bilayers as revealed by high-sensitivity differential scanning calorimetry. *Biochim. Biophys. Acta 1234*, 90−98.

(12) Somerharju, P., Virtanen, J. A., and Cheng, K. H. (1999) Lateral organization of membrane lipids. The superlattice view. *Biochim. Biophys. Acta 1440*, 32−48.

(13) McConnell, H. J., and Radhakrishman, A. (2003) Condensed complexes of cholesterol and phospholipids. *Biochim. Biophys. Acta 1610*, 159−173.

(14) Ahmed, S. N., Brown, D. A., and London, E. (1997) On the origin of sphingolipid/cholesterol-rich detergent-insoluble cell membranes: Physiological concentrations of cholesterol and sphingolipid induce formation of a detergent-insoluble, liquid-ordered lipid phase in model membranes. *Biochemistry 36*, 10944−10953.

(15) Brown, D. A., and London, E. (2000) Structure and function of sphingolipid- and cholesterol-rich membrane rafts. *J. Biol. Chem. 275*, 17221−17224.

(16) Simons, K., and Ikonen, E. (2000) How cells handle cholesterol. *Science 290*, 1721−1726.

(17) Dietrich, C., Bagatolli, L. A., Volovyk, Z. N., Thompson, N. L., Levi, M., Jacobson, K., and Graton, E. (2001) Lipid rafts reconstituted in model membranes. *Biophys. J. 80*, 1417−1428.

(18) Ikonen, E. (2001) Roles of lipid rafts in membrane transport. *Curr. Opin. Cell Biol. 13*, 470−477.

(19) Silvius, J. R. (2003) Role of cholesterol in lipid raft formation: Lessons from model systems. *Biochim. Biophys. Acta 1610*, 174−183.

(20) Gandhavadi, M., Allende, D., Vidal, A., Simon, S. A., and McIntosh, T. J. (2002) Structure, composition and peptide binding properties of detergent soluble bilayers and detergent resistant rafts. *Biophys. J. 82*, 1469−1482.

(21) Edidin, M. (2003) The state of lipid rafts: From model membranes to cells. *Annu. Rev. Biophys. Biomol. Struct. 32*, 257−283.

(22) Munro, S. (2003) Lipid rafts: Elusive or illusive? *Cell 115*, 377−388.

(23) McMullen, T. P. W., Lewis, R. N. A. H., and McElhaney, R. N. (2004) Cholesterol-phospholipid interactions, the liquid-ordered phase and lipid rafts in model and biological membranes. *Curr. Opin. Colloid Interface Sci. 8*, 459−468.

(24) Dahl, C. E., and Dahl, J. S. (1988) Cholesterol and Cell Function. In *The Biology of Cholesterol* (Yeagle, P. L., Ed.) pp 148−153, CRC Press, Inc., Boca Raton, FL.
(25) McElhaney, R. N. (1992) Membrane structure. In *Mycoplasmas: Molecular Biology and Pathogenesis* (Baseman, J. B., Finch, L. R., Maniloff, J., and McElhaney, R. N., Eds.) pp 113−155, American Society for Microbiology, Washington, DC.
(26) McElhaney, R. N. (1992) Membrane function. In *Mycoplasmas: Molecular Biology and Pathogenesis* (Baseman, J. B., Finch, L. R., Maniloff, J., and McElhaney, R. N., Eds.) pp 259−287, American Society for Microbiology, Washington, DC.
(27) Kandutsch, A. A., and Russell, A. E. (1960) Preputial gland tumor sterols. III. A metabolic pathway from lanosterol to cholesterol. *J. Biol. Chem. 235*, 2256−2261.
(28) Bloch, K. E. (1983) Sterol structure and membrane function. *CRC Crit. Rev. Biochem. 14*, 47−92.
(29) Cabrera-Vivas, B. M., Ramirez, J. C., Martinez-Aguila, L. M. R., and Kubli-Garfias, C. (2002) Theoretical assessment of the mechanisms involved in the cholesterol biosynthesis from lanosterol. *THEOCHEM 584*, 5−14.
(30) Brunetti-Pierri, N., Corso, G., Rossi, M., Ferrari, P., Balli, F., Rivasi, F., Annunziata, I., Ballabio, A., Russo, A. D., Andria, G., and Parenti, G. (2002) Lathosterolosis, a novel multiple-malformation/mental retardation syndrome due to deficiency of 3$\beta$-hydroxysteroid-$\Delta^5$-desaturase. *Am. J. Hum. Genet. 71*, 952−958.
(31) Krakowiak, P. A., Wassif, C. D., Kratz, L., Cozma, D., Korarova, M., Harris, G., Grinberg, A., Yang, Y., Hunter, A. G. W., Tsokos, M., Kelly, R. I., and Forbes, F. D. (2003) Lathosterolosis: An inborn error of human and murine cholesterol synthesis due to lathosterol 5-desaturase deficiency. *Hum. Mol. Genet. 12*, 1631−1641.
(32) Cooper, M. K., Wassif, C. A., Krakowiak, P. A., et al. (2003) A defective response to Hedgehog signaling in disorders of cholesterol biosynthesis. *Nat. Genet. 33*, 506−513.
(33) Forbes, F. D. (2003) Human malformation syndromes due to inborn errors of cholesterol synthesis. *Curr. Opin. Pediatr. 15*, 607−613.
(34) Rakheja, D., and Boriack, R. L. (2008) Precholesterol sterols accumulate in lipid rafts of patients with Smith-Lemli-Opitz syndrome and X-linked dominant chondrodysplasia punctata. *Pediatr. Dev. Pathol. 11*, 128−132.
(35) Gondre-Lewis, M. C., Petrache, H. I., Wassif, C. A., Harries, D., Parsegian, A., Porter, F. D., and Peng Loh, Y. (2006) Abnormal sterols in cholesterol-deficiency diseases cause secretory granule malformation and decreased membrane curvature. *J. Cell Sci. 119*, 1876−1885.
(36) Leppimaki, P., Mattinen, J., and Slotte, J. P. (2000) Sterol-induced upregulation of phosphatidylcholine synthesis in cultured fibroblasts is affected by the double-bond position in the sterol tetracyclic ring structure. *Eur. J. Biochem. 267*, 6385−6394.
(37) Stottrup, B. L., and Keller, S. L. (2006) Phase behavior of lipid monolayers containing DPPC and cholesterol analogs. *Biophys. J. 90*, 3176−3183.
(38) Nyholm, T. K. M., Nylund, M., and Slotte, J. P. (2003) A calorimetric study of binary mixtures of dihydrosphingomyelin and sterols, sphingomyelin, or phosphatitylcholine. *Biophys. J. 84*, 3138−3146.
(39) Ranadive, G. N., and Lala, A. K. (1987) Sterol-phospholipid interaction in model membranes: Role of C5-C6 double bond in cholesterol. *Biochemistry 26*, 2426−2431.
(40) Oradd, G., Shahedi, V., and Lindblom, G. (2009) Effect of sterol structure on the bending rigidity of lipid membranes: A $^2$H-NMR transverse relaxation study. *Biochim. Biophys. Acta 1788*, 1762−1771.
(41) Petrache, H. I., Harries, D., and Parsegian, V. A. (2005) Alteration of lipid membrane rigidity by cholesterol and its metabolic precursors. *Macromol. Symp. 219*, 39−50.
(42) Wang, X., and Quinn, P. J. (2002) Cubic phase is induced by cholesterol in the dispersion of 1-palmitoyl-2-oleoyl-phosphatidylethanolamine. *Biochim. Biophys. Acta 1564*, 66−72.
(43) Wang, J., Megha., and London, E. (2004) Relationship between sterol/steroid structure and participation in ordered lipid domains (lipid rafts): Implications for lipid raft structure and function. *Biochemistry 43*, 1010−1018.
(44) Megha., Bakht, O., and London, E. (2006) Cholesterol precursors stabilize ordinary and ceramide-rich ordered lipid domains (lipid rafts) to different degrees. Implications for the Bloch hypothesis and sterol biosynthetic disorders. *J. Biol. Chem. 281*, 21903−21913.
(45) Shahedi, V., Oradd, G., and Lindblom, G. (2006) Domain formation in DOPC/SM bilayers studied by pfg-NMR: Effect of sterol structure. *Biophys. J. 91*, 1501−2507.
(46) Mannock, D. A., Lewis, R. N. A. H., and McElhaney, R. N. (2006) Comparative calorimetric and spectroscopic studies of the effects of lanosterol and cholesterol on the thermotropic phase behavior and organization of dipalmitoylphosphatidylcholine bilayer membranes. *Biophys. J. 91*, 3327−3340.
(47) Mannock, D. A., Lewis, R. N. A. H., and McElhaney, R. N. (2008) Comparative calorimetric and spectroscopic studies of the effects of cholesterol and epicholesterol on the thermotropic phase behaviour of dipalmitoylphosphatidylcholine bilayer membrane. *Biochim. Biophys. Acta 1778*, 2190−2202.
(48) Mannock, D. A., Lewis, R. N. A. H., and McElhaney, R. N. (2010) A calorimetric and spectroscopic comparison of the effects of ergosterol and cholesterol on the thermotropic phase behavior and organization of dipalmitoylphosphatidylcholine bilayer membranes. *Biochim. Biophys. Acta 1798*, 376−388.
(49) Benesch, M. G. K., Mannock, D. A., and McElhaney, R. N. (2011) Sterol chemical configuration influences the thermotropic phase behaviour of dipalmitoylphosphatidylcholine bilayers containing 5$\alpha$-cholestan-3$\beta$- and 3$\alpha$-ol. *Chem. Phys. Lipids 164*, 62−69.
(50) Benesch, M. G. K., Mannock, D. A., and McElhaney, R. N. (2011) Sterol chemical configuration and conformation influence the thermotropic phase behaviour of dipalmitoyl-phosphatidylcholine mixtures containing 5$\beta$-cholestan-3$\beta$- and -3$\alpha$-ol. *Chem. Phys. Lipids 164*, 70−77.
(51) McMullen, T. P. W., and McElhaney, R. N. (1995) New aspects of the interactions of cholesterol and dipalmitoylphosphatidylcholine bilayers as revealed by high-sensitivity differential scanning calorimetry. *Biochim. Biophys. Acta 1234*, 90−98.
(52) Lewis, R. N. A. H., Mannock, D. A., and McElhaney, R. N. (2007) Differential scanning calorimetry in the study of lipid phase transitions in model and biological membranes: Practical considerations. In *Methods in Membrane Lipids* (Dopico, A., Ed.) pp 171−195, Humana Press, Totowa, NJ.
(53) Lewis, R. N. A. H., Winter, I., Kriechbaum, M., Lohner, K., and McElhaney, R. N. (2001) Studies of the structure and organization of cationic lipid membranes: Calorimetric, spectroscopic and X-ray diffraction studies of linear saturated P-O-ethyl phosphatidylcholines. *Biophys. J. 80*, 1329−1342.
(54) Lewis, R. N. A. H., and McElhaney, R. N. (1996) FTIR spectroscopy in the study of hydrated lipids and lipid bilayer membranes. In *Infrared Spectroscopy of Biomolecules* (Mantsch, H. H., and Chapman, D., Eds.) pp 159−202, John Wiley and Sons, New York.
(55) Linseisen, F. M., Bayerl, S., and Bayerl, T. M. (1996) $^2$H-NMR and DSC study of DPPC-DODAB mixture. *Chem. Phys. Lipids 83*, 9−23.
(56) Mannock, D. A., Lewis, R. N. A. H., McMullen, T. P. W., and McElhaney, R. N. (2010) The effect of variations in phospholipid and sterol structure on the nature of lipid−sterol interactions in lipid bilayer model membranes. *Chem. Phys. Lipids 163*, 403−448.
(57) Krivanek, R., Okoro, L., and Winter, R. (2008) Effect of cholesterol and ergosterol on the compressibility and volume fluctuations of phospholipid-sterol bilayers in the critical point region: A molecular acoustic and calorimetric study. *Biophys. J. 94*, 3538−3548.
(58) McMullen, T. P. W., Lewis, R. N. A. H., and McElhaney, R. N. (1993) Differential scanning calorimetric study of the effect of cholesterol on the thermotropic phase behavior of a homologous series of linear saturated phosphatidylcholines. *Biochemistry 32*, 516−522.

(59) McMullen, T. P. W., Lewis, R. N. A. H., and McElhaney, R. N. (1994) Comparative differential scanning calorimetric and FTIR and $^{31}$P-NMR spectroscopic studies of the effects of cholesterol and androstenol on the thermotropic phase behavior and organization of phosphatidylcholine bilayers. *Biophys. J. 66*, 741−752.
(60) McMullen, T. P. W., Lewis, R. N. A. H., and McElhaney, R. N. (1999) Calorimetric and spectroscopic studies of the effects of cholesterol on the thermotropic phase behavior and organization of a homologous series of linear saturated phosphatidylethanolamine bilayers. *Biochim. Biophys. Acta 1416*, 119−234.
(61) McMullen, T. P. W., Lewis, R. N. A. H., and McElhaney, R. N. (2000) Differential scanning calorimetric and Fourier transform infrared spectroscopic studies of the effects of cholesterol on the thermotropic phase behavior and organization of a homologous series of linear saturated phosphatidylserine bilayer membranes. *Biophys. J. 79*, 2056−2065.
(62) Mannock, D. A., McIntosh, T. J., Jang, X., Covey, D. F., and McElhaney, R. N. (2003) Effects of natural and enantiomeric cholesterol on the thermotropic phase behavior and structure of egg sphingomyelin bilayers. *Biophys. J. 84*, 1038−1046.
(63) Keller, S. L. (2003) Miscibility transitions and lateral compressibility in liquid phases of lipid monolayers. *Langmuir 19*, 1451−1456.
(64) Vilcheze, C., McMullen, T. P. W., McElhaney, R. N., and Bittman, R. (1996) The effect of side chain analogues of cholesterol on the thermotropic phase behavior of 1-stearoyl-2-oleoyl-phosphatidylcholine bilayers: A differential scanning calorimetric study. *Biochim. Biophys. Acta 1279*, 235−242.
(65) Lewis, R. N. A. H., and McElhaney, R. N. (2007) Fourier Transform infrared spectroscopy in the study of lipid phase transitions in model and biological membranes: Practical considerations. In *Methods in Membrane Lipids* (Dopico, A., Ed.) pp 207−226, Humana Press, Totowa, NJ.
(66) Lewis, R. N. A. H., and McElhaney, R. N. (1998) The structure and organization of phospholipid bilayers as revealed by infrared spectroscopy. *Chem. Phys. Lipids 96*, 9−21.
(67) Wong, P. T. T., Capes, S. E., and Mantsch, H. H. (1989) Hydrogen-bonding between anhydrous cholesterol and phosphatidylcholines: An infrared spectroscopic study. *Biochim. Biophys. Acta 980*, 37−41.
(68) Róg, T., Pasenkiewicz-Gierula, M., Vattulainen, I., and Karttunen, M. (2009) Ordering effects of cholesterol and its analogues. *Biochim. Biophys. Acta 1788*, 97−121.
(69) Israelachvili, J. N. (2011) *Intermolecular and Surface Forces*, 3rd ed., Academic Press, New York.
(70) Beattie, M. E., Veatch, S. L., Stottrup, B. J., and Keller, S. L. (2005) Sterol structure determines miscibility versus melting transitions in lipid vesicles. *Biophys. J. 89*, 1760−1768.
(71) Gopal, A., and Lee, K. Y. C. (2006) Headgroup percolation and collapse of condensed Langmuir monolayers. *J. Phys. Chem. B 110*, 22079−22087.
(72) Lintker, K. B., Kpere-Daibo, P., Fliesler, S. J., and Serfis, A. B. (2009) A comparison of the packing behavior of egg phosphatidylcholine with cholesterol and biogenically related sterols in Langmuir monolayer films. *Chem. Phys. Lipids 161*, 22−31.
(73) Garidel, P., and Blume, A. (2000) Miscibility of phosphatidylethanolamine-phosphatidylglycerol mixtures as a function of pH and acyl chain length. *Eur. Biophys. J. 28*, 629−638.
(74) Slotte, J. P. (1995) Effect of sterol structure on molecular interactions and lateral domain formation in monolayers containing dipalmitoylphosphatidylcholine. *Biochim. Biophys. Acta 1237*, 127−134.
(75) Lewis, R. N. A. H., and McElhaney, R. N. (1993) Calorimetric and spectroscopic studies of the polymorphic phase behavior of a homologous series of n-saturated 1,2-diacyl phosphatidylethanolamines. *Biophys. J. 64*, 1081−1096.
(76) Cournia, Z., Ullmann, G. M., and Smith, J. C. (2007) Differential effects of cholesterol, ergosterol and lanosterol on a dipalmitoyl phosphatidylcholine membrane: A molecular dynamics simulation study. *J. Phys. Chem. B 111*, 1786−1801.
(77) Aittoniemi, J., Róg, T., Niemelä, P., Pasenkiewicz-Gierula, M., Karttunen, M., and Vattulainen, I. (2006) Tilt: Major factor in sterols' ordering capability in membranes. *J. Phys. Chem. B. 110*, 25562−25564.
(78) Aittoniemi, J., Niemela, P. S., Hyvonen, M. J., Karttunen, M., and Vattulainen, I. (2007) Insight into the putative specific interactions between cholesterol, sphingomyelin, and palmitoyl-oleoyl phosphatidylcholine. *Biophys. J. 92*, 1125−1137.
(79) Khelashvili, G., Pabst, G., and Harries, D. (2010) Cholesterol orientation and tilt modulus in DMPC bilayers. *J. Phys. Chem. B 114*, 7524−7534.
(80) Berardi, R., Orlandi, S., and Zannoni, C. (2003) Molecular dipoles and tilted smectic formation: A Monte Carlo study. *Phys. Rev. E 67*, 041708.
(81) Watanabe, G., and Tabe, Y. (2007) Tilted and non-tilted liquid crystalline Langmuir monolayers: Analogy to bulk smectic phases. *J. Phys. Soc. Jpn. 76*, 094602.
(82) Gorecka, E., Pociecha, D., Vaupotic, N., Cepic, M., Gomola, K., and Mieczkowski, J. (2008) Modulated general tilt structures in bent-core liquid crystals. *J. Mater. Chem. 18*, 3044−3049.
(83) Archer, P., and Dierking, I. (2005) Experimental determination of the full Landau potential of bent-core doped ferroelectric liquid crystals. *Phys. Rev. E 72*, 041713.
(84) Yamane, H., Yabuuchi, Y., Fukagawa, H., Kera, S., Okudaira, K. K., and Ueno, N. (2006) Does the molecular orientation induce an electric dipole in Cu-phthalocyanine thin films? *J. Appl. Phys. 99*, 093705.
(85) Monti, O. L. A., and Steele, M. P. (2010) Influence of electrostatic fields on molecular electronic structure: Insights for interfacial charge transfer. *Phys. Chem. Chem. Phys. 12*, 12390−12400.
(86) Watanabe, G., Saito, J.-I., Kato, N., and Tabe, Y. (2011) Orientational correlations in two-dimensional liquid crystals studied by molecular dynamics simulation. *J. Chem. Phys. 134*, 054513.
(87) Moy, V. T., Keller, D. J., and McConnell, H. M. (1988) Molecular order in finite two-dimensional crystals of lipid at the air-water interface. *J. Phys. Chem. 92*, 5233−5238.
(88) Weidemann, G., and Vollhardt, D. (1996) Long-range tilt orientational order in phospholipid monolayers: A comparative study. *Biophys. J. 70*, 2758−2766.
(89) Iwamoto, M., Liu, F., and Ou-Yang, Z.-C. (2006) Shape and stability of two-dimensional lipid domains with dipole-dipole interactions. *J. Chem. Phys. 125*, 224701.
(90) Lee, D. W., Min, Y., Prajnaparamitra, D., Ramachandran, A., Israelachvili, J. N., and Zasadzinski, J. A. (2011) Relating domain size distribution to line tension and molecular dipole density in model cytoplasmic myelin lipid monolayers. *Proc. Natl. Acad. Sci. U.S.A. 108*, 9425−9430.
(91) Baginski, M., Tempczyk, A., and Borowski, E. (1989) Comparative conformational analysis of cholesterol and ergosterol. *Eur. J. Biophys. 17*, 159−166.
(92) Alwarawrah, M., Dai, J., and Huang, J. (2010) A molecular view of the cholesterol condensing effect in DOPC lipid bilayers. *J. Phys. Chem. B 114*, 7516−7523.
(93) Siu, S. W. I., Vácha, R., Jungwirth, P., and Böckmann, R. A. (2008) Biomolecular simulations of membranes: Physical properties from different force fields. *J. Chem. Phys. 128*, 125103.
(94) Patra, M., Karttunen, M., Hyvonen, M. T., Falck, E., Lindqvist, P., and Vattulainen, I. (2003) Molecular dynamics simulations of lipid bilayers: Major artifacts due to truncating electrostatic interactions. *Biophys. J. 84*, 3636−3645.
(95) Patra, M., Karttunen, M., Hyvonen, M. T., Falck, E., and Vattulainen, I. (2004) Lipid bilayers driven to a wrong lane in molecular dynamics simulations by subtle changes in long-range electrostatic interactions. *J. Phys. Chem. B 108*, 4485−4494.
(96) Rog, T., Vattulainen, I., Jansen, M., Ikonen, E., and Karttunen, M. (2008) Comparison of cholesterol and its direct precursors along the biosynthetic pathway: Effects of cholesterol, desmosterol and 7-

dehydrocholesterol on saturated and unsaturated lipid bilayers. *J. Chem. Phys. 129*, 154508.
(97) Collins, M. D., and Keller, S. L. (2008) Tuning lipid mixtures to induce or suppress domain formation across leaflets of unsupported asymmetric bilayers. *Proc. Natl. Acad. Sci. U.S.A. 105*, 124−128.
(98) Almeida, P. F. (2011) A simple thermodynamic model of the liquid-ordered state and the interactions between phospholipids and cholesterol. *Biophys. J. 100*, 420−429.
(99) Rodriguez, R. J., and Parks, L. W. (1983) Structural and physiological features of sterols necessary to satisfy bulk membrane and sparking requirements in yeast sterol auxotrophs. *Arch. Biochem. Biophys. 225*, 861−871.
(100) Rodriguez, R. J., Taylor, F. R., and Parks, L. W. (1982) A requirement for ergosterol to permit growth of yeast sterol auxotrophs on cholestanol. *Biochem. Biophys. Res. Commun. 106*, 435−441.
(101) Elliot, C. G., and Sansome, E. J. (1977) The influence of sterols on meiosis in *Phytophthora cactorum*. *J. Gen. Microbiol. 9*, 141−145.
(102) Xu, F., Rychnovsky, S. D., Belani, J. D., Hobbs, H. H., Cohen, J. C., and Rawson, R. B. (2005) Dual roles for cholesterol in mammalian cells. *Proc. Natl. Acad. Sci. U.S.A. 102*, 14551−14556.
(103) Maruyoma, S., Morisaki, M., and Ikekawa, N. (1982) Structural requirement of sterol nucleus for the silkworm growth and development. *Steroids 40*, 341−346.